Aus dem Department für Augenheilkunde Tübingen

Universitäts-Augenklinik

# BAFF, GDF-15 and Osteopontin as biomarkers in the early-metastasis of uveal melanoma

**Inaugural-Dissertation**

**zur Erlangung des Doktorgrades**

**der Medizin**

**der Medizinischen Fakultät**

**der Eberhard Karls Universität**

**zu Tübingen**

**vorgelegt von**

**Lin, Zenan**

**2021**

Dekan: Professor Dr. B. Pichler

1. Berichterstatter: Professorin. Dr. D. Süsskind

2. Berichterstatter: Privatdozentin Dr. M. Renovanz

Tag der Disputation: 24.03.2021

**To my family**

**Abbreviations**

| | |
|---|---|
| UM | Uveal melanoma |
| LFTs | Liver function tests |
| CT | Computer tomography |
| LBD | Largest basal diameter |
| BAFF | B-cell activating factor |
| BAFF-R | B-cell activating factor-receptor |
| TACI | Transmembrane activator and CAML interactor |
| OPN | Osteopontin |
| GDF-15 | Growth differentiation factor-15 |
| ELISA | Enzyme-Linked Immunosorbent Assay |
| IHC | Immunohistochemical |
| TME | Tumor microenvironment |
| FFPE | Formalin-fixed, Paraffin-embedded |
| TNM | TNM Classification of Malignant Tumors |
| ANOVA | Analysis of variance |
| MIA | Melanoma inhibitory activity |
| ROC | Receiver operating characteristic curve |
| AUC | Area under curve |

# Contents

# 1. Introduction

## 1.1 The early-metastasis of uveal melanoma

As the most common-seen primary eye cancer, uveal melanoma (UM) constitutes about 85% of the intraocular malignancies.(Krantz et al., 2017, Piperno-Neumann et al., 2019) Its incidences vary greatly in different ethnic populations. For instance, the incidence of UM was reported to be more than 10 times higher in the United States than in South Korea (5 per million VS 0.4 per million).(Krantz et al., 2017) Previous studies revealed that half of the UM patients would develop metastatic diseases. Notably, most of the metastatic lesions were firstly observed in the liver.(Piperno-Neumann et al., 2019) The liver tropism of UM metastasis still remained poorly elucidated. Less than 10% of the patients with overt clinically detected metastases were able to survive more than two years.(Krantz et al., 2017)

Due to the lack of effective therapies for the metastatic UM, it's of significance to detect the metastasis at an early stage.(Chattopadhyay et al., 2016, Carvajal et al., 2017) Thanks to the development of emerging and novel technologies such as the next generation sequencing (NGS), great advances have been achieved in the research of UM.(Robertson et al., 2017a) For example, Robertson and colleagues have performed a multi-omics' study on UM and analysed various parameters such as chromosomal copy number variations, cytogenetic alterations, DNA methylation, mRNA and LncRNA features.(Robertson et al., 2017a, Lin and Süsskind, 2020) They had successfully categorized the patients into four hierarchical prognosis-related subgroups which indicated different risk of metastasis. Nonetheless, the inefficient cost-benefit and time-consuming features make such a comprehensive multi-omics' study unfeasible to

be introduced as the routine monitoring activities to the clinic. So far, the conventional screening methods such as the liver function tests (LFTs, including aspartate aminotransferase, alanine aminotransferase, alkaline phosphatase and lactate dehydrogenase etc.), ultrasonography and computer tomography (CT) were widely used in the clinic. However, they were limited by some aspects. Prior studies showed that the LFTs not only failed to discriminate the metastasis of UM at an early timepoint but also offered a low sensitivity of 14.7%.(Mouriaux et al., 2012, Diener-West et al., 2004) Due to the limitation of resolution, the ultrasonography and CT were not able to detect the very tiny pre-metastatic niches which led to unavoidable false negative results.(Aguado et al., 2017) Moreover, these conventionally screening methods also had disadvantages in the radiation exposure and high expenses.(Eskelin et al., 1999, Hicks et al., 1998) Therefore, more feasible and efficient approaches with cheap cost are still urgently needed to address the limitations of conventional screening manners.

## 1.2 Blood-based biomarkers for the early-metastasis of UM

Though the tumor specimens will offer the valuable first-hand information of the malignancies, it is not feasible to perform the tumor biopsies regularly in the clinic due to its invasiveness and potential dissemination of malignant cells.(Shyamala et al., 2014) By contrast, blood samples can be easily acquired by minimally invasive approaches. Liotta and colleagues described the blood to be a treasure trove which contained tremendous amounts of undiscovered biomarkers. (Liotta et al., 2003) It not only supplies the nutrition and oxygen to the tumor but also transports their metabolites and secretions that manifested the dynamic pathologic states of the malignancies.(Abildgaard and Vorum, 2013b) According to Hanash and colleagues, the cancer-associated blood biomarkers were majorly generated by the malignant cells, the tumor microenvironment, the host and the interactions between them.(Hanash et al., 2011) Numerous kinds of cancers were reported to release not only the circulating

tumor cells into vasculature and disseminated to the distant regions but also various cytokines into the circulation system.(Poudineh et al., 2018) Moreover, considering the acknowledged hematogenous dissemination of UM, it's also reasonable to investigate the blood biomarkers.(Bakalian et al., 2008, Triozzi and Singh, 2012) Thus, the content rich blood could serve as a promising resource for the exploration of the status of tumors. Furthermore, its easy accessibility also enables the noninvasive screening manner for the cancer monitor. (Hanash et al., 2011)

Among a variety of methods, the analysis of the blood-based biomarkers has already been proved to be a useful prognostic tool for the metastases of many tumors.(Brown et al., 2018, Suesskind et al., 2012) Some known tumor-associated biomarkers such as CA125 (for ovarian cancer), PSA (for prostate cancer) and CA19-9 (for pancreatic cancer) were even approved by the FDA (Food and Drug Administration) and applied for longitudinal monitoring of cancers in the clinical practices.(Borrebaeck, 2017b) Besides, there are also many biomarkers which were not yet approved by FDA, however identified to be candidate tumor-related biomarkers in previous laboratory-based experiments. For example, prior studies on breast cancer showed that the concentrations of blood-based proteins ATX, CDH5, P1NP, 1-CTP and CTX were significantly upregulated after the diagnosis of metastasis. (Shao et al., 2019, Fry et al., 2016, Brown et al., 2018) They were independently regarded as promising biomarkers with the ability to detect the early-metastasis of breast cancer. Likewise, various cytokines such as MIA and PRAME were investigated in several previous researches on melanoma and demonstrated their good potential in monitoring the early-metastasis.(Bosserhoff et al., 2001, Field et al., 2016) In particular, one of our pilot studies identified that serum levels of GDF-15 were upregulated in the patients with metastasis in comparison to those without metastasis.(Suesskind et al., 2012)

## 1.3 Background of candidate blood-based biomarkers of UM

The selection of candidate biomarkers is always a big challenge because of the abundantly expressed elements within the blood. In order to save time and sample, we performed a preliminary study with a multiple cytokine array kit (Cat No: ARY022B, R&D Systems, Minneapolis, US) which targeted 105 soluble human proteins.(Lin and Süsskind, 2020) (For details refer to Figure 3.) We aimed to find the blood-based cytokines whose expression could be used to differentiate the UM patients with early-metastases from those without. According to the results, the serum levels of BAFF, OPN and GDF-15 increased after the course of metastasis which indicated that these three cytokines might be potential biomarkers for the early-metastasis of UM.

BAFF (B cell activating factor, also reported as TNFSF13B, BLyS, TALL-1 or CD257) is a member of the tumor necrosis factor (TNF) ligand family which regulates diverse immune activities, e.g. the survival, maturation, differentiation and proliferation of the B cells. (Mackay and Schneider, 2009, Lin and Süsskind, 2020, Abildgaard and Vorum, 2013b, Lied and Berstad, 2011) Previous observations already identified that the elevated serum BAFF levels were associated with the tumor invasion and metastasis of pancreatic and colorectal cancer.(Koizumi et al., 2013a, Chereches et al., 2017, Lin and Süsskind, 2020) Koizumi and colleagues indicated the range of serum BAFF in normal individuals to be 1147±315 pg/ml (Mean±SD).(Koizumi et al., 2013a, Lin and Süsskind, 2020) Besides, they confirmed that the patients with pancreatic ductal adenocarcinoma had a significantly higher level of 1704 ± 1409 pg/ml.(Koizumi et al., 2013a, Lin and Süsskind, 2020) The aforementioned multiple cytokine array using serum specimens from 4 UM patients suggested that the UM patients with metastasis had obviously higher serum BAFF concentrations than those without.(Lin and Süsskind, 2020) Strengthening the credibility of this finding, we evaluated the serum BAFF concentrations in a larger cohort of 173 UM patients from the University Eye Hospital of Tübingen and assessed their capability to differentiate the patients with metastasis

from those without.(Lin and Süsskind, 2020) The key characteristics of patients and tumors such as age, gender, tumor locations, histopathological cell types, cancer stages at diagnosis and copy number variations chromosome 3 were supplemented and analysed in this work.(Lin and Süsskind, 2020) Moreover, BAFF was previously identified to enhance the antitumor activities through interacting with various immune cells.(Shurin et al., 2016, Lin and Süsskind, 2020) This finding indicated that a brief assessment of BAFFs' role in the tumor microenvironment (TME) might be of interest since numerous immune cells appeared in the tumor tissue of UM and lymphocytic infiltration of the tumour is one of the parameters suggesting a poor prognosis.(Chandran et al., 2017, Lin and Süsskind, 2020)

OPN (Osteopontin, also reported as BSP-1, BNSP, ETA-1, SPP1 or Ric), an acidic arginine-glycine-aspartate-containing adhesive glycoprotein, a bone sialoprotein as well as a bone matrix protein, participated not only in the bone system but also in cancer-associated pathways.(Rangaswami et al., 2006) In details, OPN played a role in the tumorigenesis, metastasis and immune response in varied malignancies, such as lung, liver, bladder, gastric, colon and ovarian cancer.(Zhao et al., 2018b) With regard to uveal melanoma, OPN's role in the metastasis of UM was also analysed by several studies. Previous investigations conducted by three independent groups showed that the blood-based OPN levels were significantly higher in the metastatic UM patients than in nonmetastatic patients. (Kadkol et al., 2006, Haritoglou et al., 2009b, Reiniger et al., 2007) According to Reiniger and colleagues, normal individuals had a median plasma OPN level of 54.6 ng/ml.(Reiniger et al., 2007) In comparison, the UM patients without metastasis had a median value of 46.78 ng/ml and those with metastasis had increased median concentration of OPN of 170.72 ng/ml.(Reiniger et al., 2007) Nevertheless, these studies also had limitations. First, the sizes of enrolled UM patients in these three studies were small, with the numbers of participating patients to be 52 (15 with metastasis VS 37 without metastasis), 32 (14 with metastasis VS 18 without metastasis) and 27 (8 with metastasis VS 19 without metastasis), respectively. Hence, the validation

of their findings in a larger patient cohort is still needed.(Kadkol et al., 2006, Haritoglou et al., 2009b, Reiniger et al., 2007) Second, the associations between the expression of OPN and critical clinicopathological features of UM (e.g. histopathological cell types, copy number variations of chromosome 3, metastatic burden and etc.) were not assessed in these pilot studies. Therefore, these clinical parameters were supplemented in this study and their relations with the plasma OPN levels were rigorously analysed. Third, though previous researchers concluded that OPN was a promising biomarker for the early-metastasis of UM, they didn't evaluate the performance of plasma OPN in discriminating the UM with metastasis from those without and provide a cutoff value of plasma OPN which was significant in the clinical practices.(Kadkol et al., 2006, Haritoglou et al., 2009b, Reiniger et al., 2007) Addressing these, our current work will assess the prognostic ability of OPN and then offer a cutoff value of plasma OPN which may be utilized as a useful reference standard in the clinic.

GDF-15 (Growth Differentiation Factor 15, also known as GDF15, MIC-1, MIC1, NAG-1, PDF, PLAB, PTGFB or TGF-PL) is a member of the TGF-ß superfamily.(Emmerson et al., 2018) It was reported to regulate the cellular activities such as cell survival, differentiation, proliferation, migration and apoptosis.(Bootcov et al., 1997, Emmerson et al., 2018) In normal physiology, GDF-15 was majorly expressed in the placenta, and its enhanced expression was also observed in other organs in the context of inflammatory responses and tumor-associated processes.(Wallin et al., 2011) For instance, the expression of serum GDF-15 was identified to be significantly higher in patients with colorectal or prostate cancers than in healthy controls.(Li et al., 2016, Windrichova et al., 2017) Three previous studies reported the serum GDF-15 level of healthy individuals to be 169.24 ± 82.96 pg/ml (Mean±SD), 387.0 ± 4.2 pg/ml and 506.2 ± 258.4 pg/ml, respectively. (Zhao et al., 2019, Wang et al., 2016a, Tsai et al., 2015) One of our prior studies showed that significantly higher GDF-15 levels were observed in UM patients with clinically detectable metastases than in those without. (Suesskind et al., 2012) In the present work, we added the information of several key

clinicopathological characteristics and explored their associations with serum GDF-15 levels. In addition, in this study, we will also calculate the previously unreported cutoff value for serum GDF-15 levels in distinguishing the metastatic patients.

Last, we embarked on a study with the multiple biomarkers' panel consisting of blood-based BAFF, OPN and GDF-15 and determined whether this combination model outperformed single biomarkers. Since the mechanism underlying the metastasis is complex and numerous elements participated in this process, the clinical utility of single biomarker on identifying the early-metastases of UM has inherent limitations. A panel consisting of multiple biomarkers may better reflect the complexity of metastasis and offer better performance in differentiating the UM patients with early-metastases from those without.

## 1.4 Aims of the study

We wanted to assess whether the blood-based levels of BAFF, GDF-15 and OPN could be utilized as promising biomarkers for the early-detection of metastasis of UM.

Besides, we would also evaluate the performance of a combination mode of these three cytokines and determine whether the combination method had a better performance than utilizing single biomarker.

# 2. Materials and methods

## 2.1 Patient enrollment and eligibility criteria

173 patients with diagnosed UM and treated in the University Eye Hospital of Tübingen were included in this study. The enrollment and eligibility criteria for participants were in accordance with the inclusion and exclusion criteria described in our previous papers.(Suesskind et al., 2012, Lin and Süsskind, 2020) Briefly, those who were older than 18 years and with the ability to give consent to participate in this project were regarded as eligible participants.(Suesskind et al., 2012, Lin and Süsskind, 2020) Besides, those who demonstrated an active second malignancy were removed from our study.(Suesskind et al., 2012, Lin and Süsskind, 2020) The study followed the Declaration of Helsinki as revised in Tokyo and Venice, and was approved by the local ethics committee (449/2018BO2).(Lin and Süsskind, 2020)

A control group composed of 7 healthy men and 16 healthy women was also introduced to this study and their blood samples were acquired after a consent was made. The control group had a median age of 49 years (ranging from 22 to 78 years).(Lin and Süsskind, 2020)

## 2.2 Definition of tumor characteristics

TNM size stratification and TNM staging of UM was conducted according to the 8$^{th}$ edition of the AJCC (American Joint Committee on Cancer) cancer staging manual.(Amin et al., 2017, Lin and Süsskind, 2020) (see Figure 1. and Table 1.) Largest basal diameter (LBD) and apical height of the primary tumors were measured with sonography or MRI.(Lin and Süsskind, 2020) Metastatic burden was estimated as diameter of the largest metastasis in cm.(Lin and Süsskind, 2020)

The definition of tumor location could be summarized as follows: anterior, i.e. ciliary body melanomas; peripheral, i.e. those located between the ciliary body and the equator; posterior, i.e. those situated behind the equator of the eye.(Lin and Süsskind, 2020)

The time interval between the first and the last blood acquisition was seen as the follow up period.

Cytogenetic results concerning chromosome 3 copy number variation of 41 patients and histopathological cell types (i.e. epithelioid, spindle and mixed cell types) of 50 patients have been acquired from the clinical data bank of University Eye Hospital of Tübingen.(Lin and Süsskind, 2020) The clinicopathological features of the 173 patients were compiled in Table 3.(Lin and Süsskind, 2020)

| **Apical height (mm)** | | | | | | | |
|---|---|---|---|---|---|---|---|
| >15.0 | 4 | 4 | 4 | 4 | 4 | 4 | 4 |
| 12.1-15.0 | 3 | 3 | 3 | 3 | 3 | 4 | 4 |
| 9.1-12.0 | 3 | 3 | 3 | 3 | 3 | 3 | 4 |
| 6.1-9.0 | 2 | 2 | 2 | 2 | 3 | 3 | 4 |
| 3.1-6.0 | 1 | 1 | 1 | 2 | 2 | 3 | 4 |
| ≤3.0 | 1 | 1 | 1 | 1 | 2 | 2 | 4 |
| | ≤3.0 | 3.1-6.0 | 6.1-9.0 | 9.1-12.0 | 12.1-15.0 | 15.1-18.0 | >18.0 |
| **Largest basal diameter (mm)** | | | | | | | |

Figure 1. Classification of ciliary and choroid uveal melanoma based on thickness and diameter. (Note: This figure was reproduced according to the 8th AJCC cancer staging manual. (Amin et al., 2017))

Table 1. The cancer staging of uveal melanoma.

| Stages | T (Tumor) | N (Lymph nodes) | M (Metastasis) |
|---|---|---|---|
| **I** | T1a | N0 | M0 |
| **IIA** | T1b-d | N0 | M0 |
| **IIA** | T2a | N0 | M0 |
| **IIB** | T2b | N0 | M0 |
| **IIB** | T3a | N0 | M0 |
| **IIIA** | T2c-d | N0 | M0 |
| **IIIA** | T3b-c | N0 | M0 |
| **IIIA** | T4a | N0 | M0 |
| **IIIB** | T3d | N0 | M0 |
| **IIIB** | T4b-c | N0 | M0 |
| **IIIC** | T4d-e | N0 | M0 |
| **IV** | Any T | N1 | M0 |
| **IV** | Any T | Any N | M1a-c |

Note: this table was reproduced according to the 8th AJCC cancer staging manual. (Amin et al., 2017)

## 2.3 Blood acquisition

### 2.3.1 Serum preparation

The blood specimens of participants were acquired and prepared similarly to our formerly described methods. (Suesskind et al., 2012) Conventionally, the interval of patient visits was set to 6 months. At each visit, 15 ml blood was taken from each patient and divided evenly into 2 samples. After standing for 30 mins at room temperature, blood samples were centrifuged for 30 mins at 2200 × g. In order to get rid of the residual blood cells, the supernatant was aspirated into 1.5 ml microfuge tubes for the second centrifugation. The resulting supernatant was distributed into 0.5 ml tubes and stored at −80°C refrigerator.

### 2.3.2 Plasma preparation

Blood samples were distributed into EDTA-treated tubes. Blood samples were centrifuged for 30 mins at 2200 × g. In order to deplete the platelets, the supernatant was aspirated into 1.5 ml microfuge tubes for the second centrifugation. The plasma samples were apportioned into 0.5 ml aliquots and stored at −80°C in the refrigerator.

## 2.4. Multiple cytokines array test and quantification

With the Human XL Cytokine Array Kit (Cat No.: ARY022B, R&D Systems, Minneapolis, US), we conducted the multiple cytokines array tests by using four serum specimens from UM patients and two from normal individuals. A buffered protein base with preservatives was utilized as block buffer in each well of a 4-well multi-dish.

Afterwards, four nitrocellulose membranes each carrying multiple capture antibodies were placed in a separate well and then incubated on a rocking platform shaker for 60 mins. After aspirating the block buffer, 1.5 ml prepared serum were added to each well. The multi-dish was placed on the rocking shaker again and incubated overnight at a temperature of 4 °C. On the next day, we moved the membranes to separated plastic containers with 20 ml of wash buffer and rinsed the multi-dish with distilled water. Then, the membranes were placed back to each well and washed by wash buffer for 10 mins on the shaker. This process was repeated for two times. After washing, 1.5 ml of prepared detection antibody cocktail was added to each well of the multi-dish and incubated for 60 mins on the shaker. Later, the membranes went through the abovementioned washing processes. 2.0 ml of Streptavidin-HRP were pipetted to each well of the multi-dish and incubated for 30 mins at room temperature on the shaker. Afterwards, the membranes went through the washing processes as described before. In order to make the membranes dry, their lower edges were blotted on paper towels and then placed on the bottom sheets of the plastic sheet protectors. We added 1.0 ml of the prepared Chemi Reagent Mix to each membrane and then covered them with the top plastic sheet. The air bubbles were smoothed out to make sure that all areas of the membranes were filled up by the Chemi Reagent Mix and incubated for 1 min. The paper towels were used to absorb the retaining Chemi Reagent Mix from the sides of plastic sheets. The membranes were then covered with plastic wrap and exposed for 2 mins in the chemiluminescent channel of an imaging system (Odyssey imaging system, LI-COR Bioscience, Lincoln, US). By using the software of Image Studio™ Lite (version 5.2.5, LI-COR Biosciences, Lincoln, US), we measured the densities of each spot of the film which represented the levels of corresponding cytokines.

## 2.5. Evaluation of the levels of serum BAFF and GDF-15

Serum samples were diluted and examined in duplicate per each assay according to the manufacturers´ instructions. Then, BAFF and GDF-15 were analysed by the Human Premixed Multi-Analyte Kit (Kit Lot Number: L123335) of Magnetic Luminex Assay (Kit Cat No.: LXSAHM-03) following the manufacturer instructions.(Lin and Süsskind, 2020) Quantitative evaluation of serum BAFF and GDF-15 levels was conducted in a Luminex MAGPIX system (Luminex Corporation, Austin, TX, USA).(Lin and Süsskind, 2020) A 5-parameter logistic curve-fitting method was introduced to calculate the concentrations of BAFF and GDF-15. We also recorded the time points at which sera were acquired. The first serum specimen in the non-metastatic patients and the first serum sample after diagnosis of metastasis in the metastatic patients were evaluated.(Lin and Süsskind, 2020)

## 2.6. Evaluation of the levels of plasma OPN

Previously, a study on epithelial malignant pleural mesothelioma indicated that the levels of plasma OPN is more stable than serum OPN.(Cristaudo et al., 2010) Therefore, in this work, we measured the concentration of plasma OPN instead of serum OPN. The commercial available Elisa kit (Cat No.: DOST00, R&D Systems, Minneapolis, USA) was used to test the plasma OPN levels in this study. According to the manufacturer's manual, we reconstituted the standard of plasma OPN with distilled water and made the standard series. The plasma samples were diluted 1:30 before the evaluation. 100 µl of a buffered protein base with preservatives (Assay Diluent RD1-6) were pipetted to each well of a 96-well polystyrene microplate. Then, we added 50 µl of diluted plasma of UM patients and healthy controls, and standard series to each well and then covered the plate with a provided strip. The 96-well microplate was incubated for 120 mins at room temperature. Afterwards, the liquid within each well was absorbed and throwed away

before being washed for 4 times by 400 µl wash buffer per well. Ultimately, the excess wash buffer within each well was aspirated. In order to make the wells dry, we inverted the microplate against paper towels. After adding 200 µl of Human OPN Conjugate to each well, we covered the plate with a new strip and incubated it for another 120 mins at room temperature. After the incubation, a washing process was repeated for 4 times similar as described above. We pipetted 200 µl of prepared substrate solution to each well and incubated it for 30 mins (protect from light) at room temperature. Finally, 50 µl of stop solution were added to each well to stop the interactions. We then measured the optical density of each well with a reader (Infinite 200, TECAN, Zürich, Switzerland) which had the wavelength set to 450 nm and the corrected wavelength set to 540 nm. Then, we generated the standard curve by using a 4-parameter logistic curve-fitting approach and calculated the plasma OPN levels of tested samples.

## 2.7. Immunohistochemical staining of BAFF, BAFF-R and TACI in the UM specimens

Immunohistochemical (IHC) staining for BAFF, BAFF-R and TACI expression was performed for 50 UM tumor samples acquired from enucleations and tumor resections within the 173 patients.(Lin and Süsskind, 2020) Formalin-fixed, paraffin-embedded (FFPE) UM tissues were deparaffinized in xylol and rehydrated in a graded alcohol series.(Lin and Süsskind, 2020) We used Tris-EDTA (pH 9.0) for BAFF and BAFF-R and Citrate buffer (pH 6.0) in the case of TACI to unmask the antigen and employed the kits (ImmPRESSTM-AP REAGENT Anti-Mouse IgG, Cat. No.:MP-5402, Vector Laboratories, Burlingame, USA and ImmPRESSTM-AP REAGENT Anti-Rabbit IgG, Cat. No.:MP-5401, Vector Laboratories, Burlingame, USA) for the following processes.(Lin and Süsskind, 2020) Each section was incubated with BIOXALL (Cat. No.: SP-6000, Vector Laboratories, Burlingame, USA) to block the endogenous enzyme

activities.(Lin and Süsskind, 2020) The section was washed for three times with TBS with 0.5% Tween.(Lin and Süsskind, 2020) The section was processed with 2.5% normal horse serum. As primary antibodies, a monoclonal mouse anti-BAFF antibody was used at a dilution of 1:600 (Cat. No.: ab16081, Abcam, Cambridge, UK), a monoclonal rabbit anti-BAFF-R antibody was used at a dilution of 1:250 (Cat. No.: ab188868, Abcam, Cambridge, UK), and a monoclonal rabbit anti-TACI antibody was used at a dilution of 1:400 (Cat. No.: ab79023, Abcam, Cambridge, UK).(Lin and Süsskind, 2020) The primary antibodies were incubated at a temperature of 37℃ for 30 mins. The sections were washed three times with TBS buffer with Tween and then incubated for 30 mins with the ImmPRESSTM-AP Reagent (Horse Anti-Mouse IgG for BAFF, Horse Anti-rabbit IgG for BAFF-R and TACI).(Lin and Süsskind, 2020) Immunoreaction was visualized by using kits (ImmPACTTM Vector® Red, Alkaline Phosphatase, Cat. No.: SK-5105, Vector Laboratories, Burlingame, USA) resulting in a red colour precipitation.(Lin and Süsskind, 2020) The sections were washed three times by normal water and then counterstained for 25 seconds with hematoxylin (Cat. No.: H-3404, Vector Laboratories, Burlingame, USA).(Lin and Süsskind, 2020) The sections were washed three times again by normal water and then washed by 96% alcohol for two times, 99% alcohol for another two times.(Lin and Süsskind, 2020) Then they were processed in xylol for four times. Ultimately, the sections were mounted with Merkoglas (Merck, Darmstadt, Germany).(Lin and Süsskind, 2020) Bowel tissue was applied for positive control staining while the FFPE UM tissues which underwent the IHC procedure without primary antibody acted as negative controls.(Lin and Süsskind, 2020)

## 2.8. Quantification of BAFF, BAFF-R and TACI in the UM specimens

With a microscope (set at 500×, VHX-5000, Keyence, Osaka, Japan), we examined the staining of BAFF and assigned a percentage score of 0 (no staining), 1 (<10% of tumor cells staining), 2 (10%-50%) or 3 (50%-80%) within selected tumor areas of each slide.(Rizzardi et al., 2012, Lin and Süsskind, 2020) An intensity score was determined by the same person with 0 for no staining, 1 for weak staining, 2 and 3 for moderate and strong staining, respectively.(Lin and Süsskind, 2020) Tumor IHC score was generated by multiplication of the percentage and intensity scores.(Lin and Süsskind, 2020) A representative number of areas for the tumors of different sizes were chosen to cover the whole tumor tissue and a solid Tumor IHC score was generated for each area.(Lin and Süsskind, 2020) In the end, the mean value of these Tumor IHC scores of BAFF was calculated for each slide.(Lin and Süsskind, 2020) In addition to tumor cells, we also marked the slides which contained tumor-infiltrating lymphocytes (TILs) which were positively stained by BAFF.(Lin and Süsskind, 2020) Herein, the widely applied grading system (i.e. Absent, Non-brisk and Brisk) developed by Clark and colleagues for the TILs in melanoma was applied to categorize the TILs in the tested specimens.(Clark Jr et al., 1989, Lin and Süsskind, 2020) (see Table 2. And Figure 2.) Besides, we also analysed the 50 IHC slides of BAFF-R and TACI and found that in every positively stained slide only a minor amount of tumor cells (approximately less than 10% of all tumor cells) presented the staining of BAFF-R and TACI.(Lin and Süsskind, 2020) This result indicated the inapplicability to employ the same analyzing approach applied in the aforementioned IHC study of BAFF which required a grading system of percentage score of tumor cells.(Lin and Süsskind, 2020) Therefore, in the IHC study of BAFF-R and TACI, we only recorded the binary staining results (i.e. positive or negative) of each slide.(Lin and Süsskind, 2020)

Table 2. Categories of TILs in melanoma. (Clark et al.(Abildgaard and Vorum, 2013a))

| Categories of TILs | Definition |
|---|---|
| Absent | The lymphocytes were not present or not directly infiltrating the tumor |
| Non-brisk | The TILs noted in one or more foci of the vertical growth phase |
| Brisk | The TILs were present throughout the substance of the vertical growth phase or present and infiltrating across the entire base of the vertical growth phase |

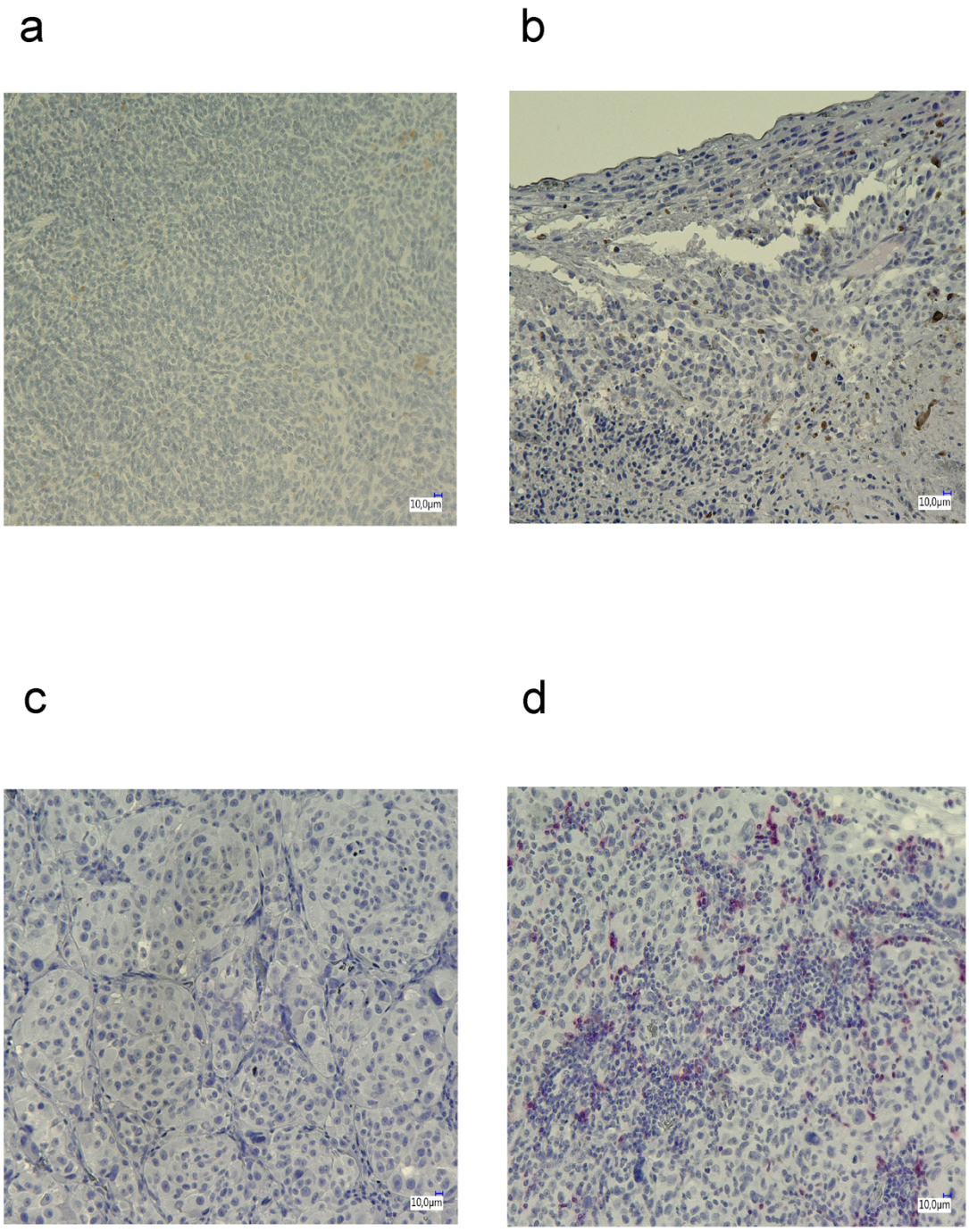


**Figure 2.** (a) Examples showing the absent category of TILs in uveal melanoma; (b-c) Examples showing the non-brisk category of TILs in uveal melanoma. These two photomicrographs were captured in one tumor specimen, while the focal TILs were seen in the marginal area (b), rare TILs were observed in the central part of the tumor (c); (d) Examples showing the brisk category of TILs in uveal melanoma.

## 2.9. Immunohistochemical staining and evaluation of CD3, CD4, CD8 and CD20 in the UM specimens

IHC staining for CD3 (marker for T cells), CD4 (marker for CD4+ T cells), CD8 (marker for CD8+ T cells) and CD20 (marker for B cells) expression was conducted for 6 UM tumor samples which were identified to have BAFF staining in the brisk category of TILs.(Lin and Süsskind, 2020) Formalin-fixed, paraffin-embedded UM tissues were deparaffinized in xylol and rehydrated in a graded alcohol series.(Lin and Süsskind, 2020) We used Citrate buffer (pH 6.0) for CD3, CD8 and CD20 and Tris-EDTA (pH 9.0) in the case of CD4 to unmask the antigen and employed the kits (ImmPRESSTM-AP REAGENT Anti-Rabbit IgG, Cat. No.:MP-5401, Vector Laboratories, Burlingame, USA and ImmPRESSTM-AP REAGENT Anti-Mouse IgG, Cat. No.:MP-5402, Vector Laboratories, Burlingame, USA) for the following processes.(Lin and Süsskind, 2020) Each section was incubated with BIOXALL (Cat. No.: SP-6000, Vector Laboratories, Burlingame, USA) to block the endogenous enzyme activities. The sections were washed for three times with TBS with 0.5% Tween.(Lin and Süsskind, 2020) The sections were processed with 2.5% normal horse serum. As primary antibodies, a monoclonal rabbit anti-CD3 antibody was used at a dilution of 1:1000 (Cat. No.: ab5690, Abcam, Cambridge, UK), a monoclonal rabbit anti-CD4 antibody was used at a dilution of 1:3000 (Cat. No.: ab133616, Abcam, Cambridge, UK), a monoclonal mouse anti-CD8 antibody was used at a dilution of 1:200 (Cat. No.: M-7103, Dako, Agilent, Santa Clara, USA) and a monoclonal mouse anti-CD20 antibody was used at a dilution of 1:500 (Cat. No.: M-0755, Dako, Agilent, Santa Clara, USA).(Lin and Süsskind, 2020) The former two primary antibodies were incubated at room temperature for 30 mins while the latter two were incubated at 37℃ for 30 mins. The sections were washed three times with TBS buffer with Tween and then incubated for 30 mins with ImmPRESSTM-AP Reagent (Horse Anti-rabbit IgG for CD3 and CD4, Horse Anti-Mouse IgG for CD8 and CD20).(Lin and Süsskind, 2020) Immunoreaction

was visualized by using kits (ImmPACTTM Vector® Red, Alkaline Phosphatase, Cat. No.: SK-5105, Vector Laboratories, Burlingame, USA) resulting in a red colour precipitation.(Lin and Süsskind, 2020) The sections were washed three times by normal water and then counterstained for 25 seconds with hematoxylin (Cat. No.: H-3404, Vector Laboratories, Burlingame, USA).(Lin and Süsskind, 2020) The sections were washed three times again by normal water and then washed by 96% alcohol for two times, 99% alcohol for another two times.(Lin and Süsskind, 2020) Then they were processed in xylol for four times. In the end, the sections were mounted with Merkoglas (Merck, Darmstadt, Germany). Bowel tissue was applied for positive control staining while the FFPE UM tissues which underwent the IHC procedure without primary antibody acted as negative controls.(Lin and Süsskind, 2020) With a microscope (set at 500×, VHX-5000, Keyence, Osaka, Japan), we examined the staining of these four proteins and recorded the binary staining results (i.e. positive or negative) of TILs of each slide.(Lin and Süsskind, 2020)

## 2.10. Statistics

Statistical analysis was conducted with GraphPad Prism (version 6.0c, GraphPad Software) and SPSS (version 25, IBM). For all statistical evaluations, a *P* value less than 0.05 was regarded as statistically significant.(Lin and Süsskind, 2020)

# 3. Results

## 3.1 Preliminary study

a

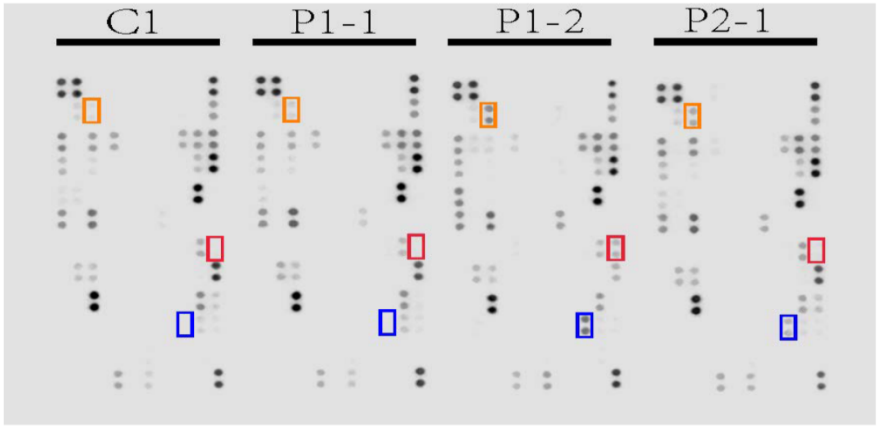


| | C1 | P1-1 | P1-2 | P2-1 | P1-2/P1-1 |
|---|---|---|---|---|---|
| BAFF | 0.0006 | 0.0009 | 0.0109 | 0.0028 | 12.1111 |
| OPN | 0.0028 | 0.0049 | 0.0209 | 0.0116 | 4.2653 |
| GDF-15 | 0 | 0.0015 | 0.0260 | 0.0095 | 17.3333 |

b

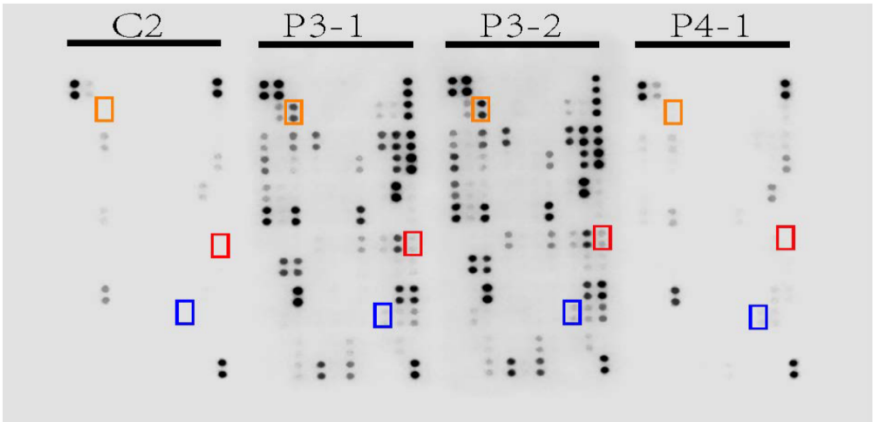


| | C2 | P3-1 | P3-2 | P4-1 | P3-2/P3-1 |
|---|---|---|---|---|---|
| BAFF | 0 | 0.0017 | 0.0041 | 0 | 2.4118 |
| OPN | 0 | 0.0132 | 0.0183 | 0 | 1.3864 |
| GDF-15 | 0 | 0.0014 | 0.0030 | 0.0020 | 2.1429 |

BAFF OPN GDF-15

**Figure 3.** (a) Multiple cytokine array analyses with serum samples from healthy control 1 (C1), UM patient 1 before diagnosis of metastasis (P1-1) , patient 1 after diagnosis of metastasis (P1-2) and patient 2 before diagnosis of metastasis (P2-1); (b) Multiple cytokine array analyses with serum samples from healthy control 2 (C2), patient 3 before diagnosis of metastasis (P3-1) , patient 3 after diagnosis of metastasis (P3-2) and patient 4 before diagnosis of metastasis (P4-1).

According to the manufacturer's manual, the signal at each spot corresponded to the amount of relevant protein bound. We measured the signals and found that the blood-based levels of BAFF, OPN and GDF-15 in the UM patient (P1) were increased after the diagnosis of metastasis with an increasing fold to be 12.1, 4. 3 and 17.3, respectively. (see Figure 3.a) Similarly, in the other UM patient P3, the expression of these three cytokines were also identified to be upregulated after the clinical detection of overt metastasis. (see Figure 3.b)

## 3.2 Patients and tumor characteristics

**Table 3. Clinicopathological features of patients and tumor**

| | Patients with metastasis | Patients without metastasis |
|---|---|---|
| Total | n=36 | n=137 |
| Sex, n (%) | 36 patients available | 137 patients available |
| Male | 15 (41.7%) | 64 (46.7%) |
| Female | 21 (58.3%) | 73 (53.3%) |
| Age at enrollment time (years) | 36 patients available | 137 patients available |
| Median (range) | 65.5 (43-79) | 67 (28-84) |
| Staging at diagnosis, n (%) | 36 patients available | 129 patients available |
| Stage I | 2 (5.6%) | 46 (35.7%) |

| | | |
|---|---|---|
| Stage II | 23 (63.9%) | 71 (55.0%) |
| Stage III | 7 (19.4%) | 12 (9.3%) |
| Stage IV | 4 (11.1%) | 0 (0%) |
| Largest basal diameter (mm) | 36 patients available | 130 patients available |
| Median (range) | 14.8 (8.1-21.5) | 11.1 (5.0-21.4) |
| Apical height (mm) | 36 patients available | 132 patients available |
| Median (range) | 6.1 (2.6-13.4) | 3.8 (1.0-18) |
| Location, n (%) | 35 patients available | 130 patients available |
| Posterior UM | 25 (71.4%) | 93 (71.5%) |
| Anterior UM | 2 (5.7%) | 4 (3.1%) |
| Peripheral UM | 8 (22.9%) | 33 (25.4%) |
| Cytogenetic alterations, n (%) | 12 patients available | 29 patients available |
| Monosomy 3 | 12 (100%) | 11 (37.9%) |
| Disomy 3 | 0 (0%) | 18 (62.1%) |
| Histopathological cell type, n (%) | 16 patients available | 34 patients available |
| Spindle | 4 (25.0%) | 21 (61.8%) |
| Epitheloid | 2 (12.5%) | 5 (14.7%) |
| Mixed | 10 (62.5%) | 8 (23.5%) |
| Categories of TILs, n (%) | 16 patients available | 34 patients available |
| Absent | 6 (37.5%) | 12 (35.3%) |
| Non-brisk | 7 (43.8%) | 13 (38.2%) |
| Brisk | 3 (18.7%) | 9 (26.5%) |

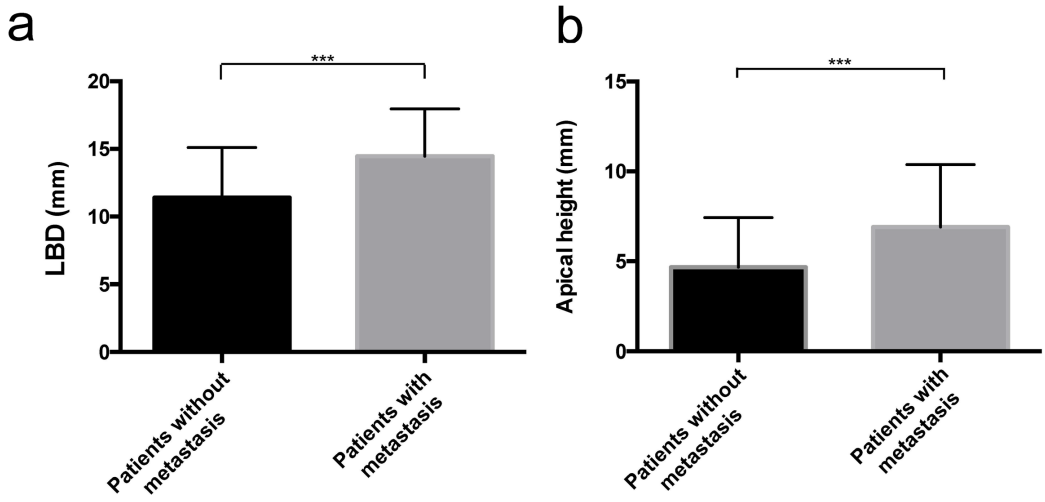


**Figure 4.** (a, b) The comparison of LBD and apical heights between patients without and those with metastasis, respectively.

Note: *** means $P<0.01$.

36 UM patients with and 137 without metastasis were selected for this study.(Lin and Süsskind, 2020) Patients' clinicopathological features are summarized in Table 3. No statistically significant differences were observed in the gender distribution between these two groups of patients.(Lin and Süsskind, 2020) Though the patients without metastasis presented a wider range of age distribution (from 28 to 84 years old) than those with metastasis (from 43 to 79 years old), the median age of both groups was quite similar (65.5 VS 67 years).(Lin and Süsskind, 2020) With respect to the cancer stages at diagnosis, the patients with metastasis had obviously higher percentages of stages II, III and IV than those without metastasis. 64% of the analysed 50 UM specimens (16 from metastatic patients and 34 from those without metastasis) contained TILs.(Lin and Süsskind, 2020) (see Table 3.) The comparison of tumor sizes revealed that the patients with metastasis had larger median tumor apical height (6.1 mm VS 3.8 mm) and LBD (14.8 mm VS 11.0 mm) than those without metastasis, respectively.(Lin

and Süsskind, 2020) Besides the median value, the mean values of apical height (6.6 mm VS 4.8 mm) and LBD (14.4 mm VS 11.4 mm) in the patients with metastasis were also significantly higher than those without metastasis. (both $P<0.01$, see Figure 4.)(Lin and Süsskind, 2020)

## 3.3 Blood-based BAFF, OPN and GDF-15 levels and early-metastasis

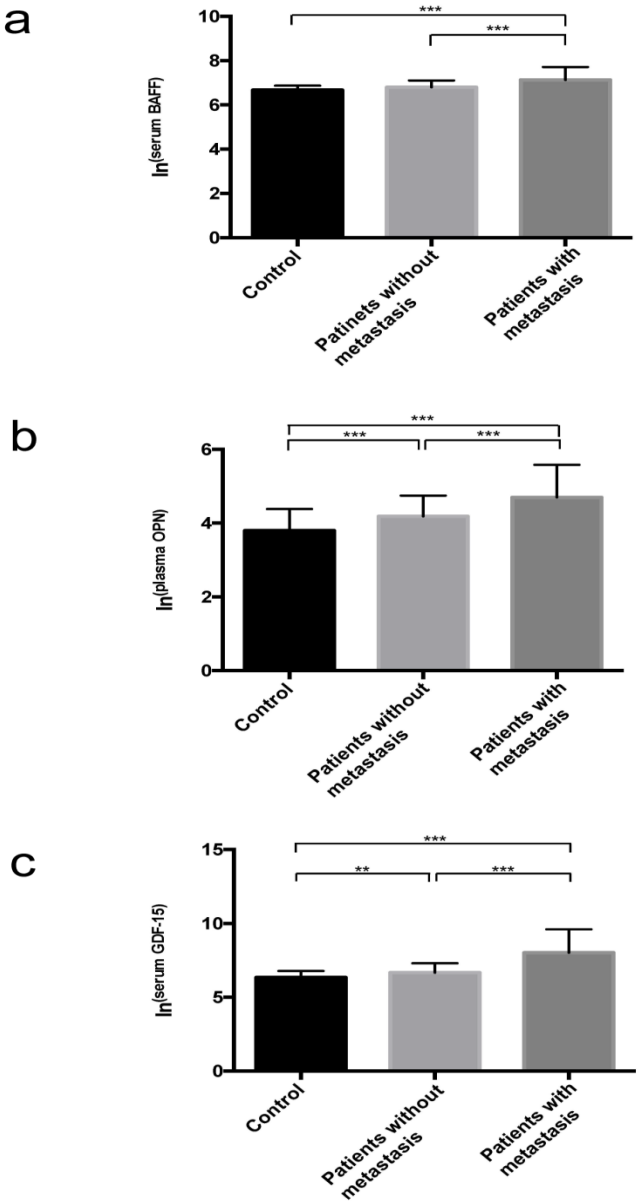


**Figure 5.** (a-c) The comparison of $ln^{(serum\ BAFF)}$, $ln^{(plasma\ OPN)}$ and $ln^{(serum\ GDF\text{-}15)}$ among control individuals, patients without and those with metastasis, respectively.

The median serum BAFF concentrations in healthy individuals, patients with and without metastasis were 809.5 pg/ml (ranging from 430.2 to 1037.2 pg/ml), 1043.1 pg/ml (from 605.5 to 6009.8 pg/ml) and 895.1 pg/ml (from 423.8 to 5969.1 pg/ml), respectively. Since the original data was not normally distributed, we performed the natural logarithm transformation of the blood-based levels of these three cytokines and generated $\ln^{(\text{serum BAFF})}$, $\ln^{(\text{plasma OPN})}$ and $\ln^{(\text{serum GDF-15})}$ for further analyses. ANOVA and Tamhane post hoc analysis proved that the $\ln^{(\text{serum BAFF})}$ in metastatic patients were significantly higher than in those without metastasis and control individuals.(both $P<0.01$, see Figure 5.a) With regards to plasma OPN, we found that the median plasma OPN levels of healthy subjects, patients with and without metastasis were 44.06 ng/ml (ranging from 16.47 to 131.1 ng/ml), 100.3 ng/ml (from 9.9 to 916.8 ng/ml), 70.1 ng/ml (from 13.4 to 318.7 ng/ml), respectively. The statistical analysis also indicated the significant higher levels in metastatic patients than in non-metastatic patients. (see Figure 5.b) Besides, the patients without metastasis were also identified to have higher concentrations of plasma OPN than healthy individuals. Similar to BAFF and OPN, the serum GDF-15 levels in patients with metastasis were also remarkably higher in the metastatic patients than in those without metastatic lesions.(see Figure 5.c) The median serum GDF-15 levels in healthy controls, metastatic patients and non-metastatic patients were 540.7 pg/ml (ranging from 264.1 to 2644.7 pg/ml), 1681.3 pg/ml (from 239.7 to 184092.3 pg/ml), 772.9 pg/ml (from 248.9 to 36637.7 pg/ml), respectively. (see Figure 5.c)

## 3.4 Correlations between blood-based BAFF, OPN and GDF-15 levels and the tumor sizes of primary and metastatic UM lesions

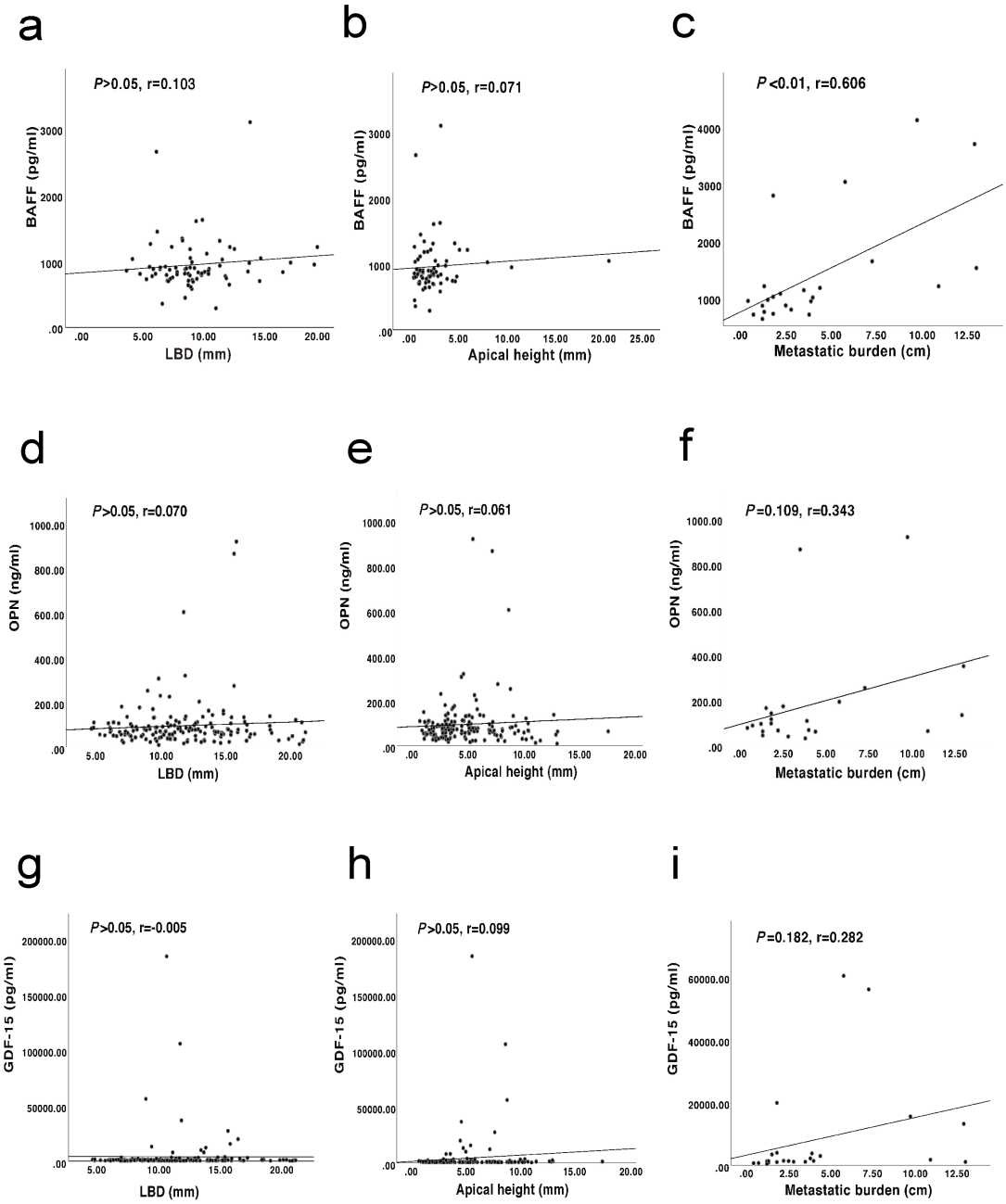

**Figure 6.** (a-c) The Pearson's correlations between serum BAFF levels and tumor LBD, apical height and metastatic burden, respectively; (d-f) The Pearson's correlations between plasma OPN levels and tumor LBD, apical height and metastatic burden, respectively; (g-i) The Pearson's correlations between serum GDF-15 levels and tumor LBD, apical height and metastatic burden, respectively.

No close associations between blood-based BAFF, OPN and GDF-15 levels and primary tumor sizes (LBD and apical height) were found in our work (all $P>0.05$, r ranges from 0.005 to 0.103, see Figure 6.a-b, d-e, g-h), while metastatic burden displayed a significant strong correlation with the serum BAFF expression. ($P<0.01$, Pearson' r=0.606, see Figure 6.c) Besides, our analysis also demonstrated weak correlations of the plasma OPN (r=0.343, $P=0.109$) and serum GDF-15 levels (r=0.282, $P=0.182$) with the metastatic burden. (see Fig. 6.f and i)

## 3.5 Serum BAFF levels and clinicopathological features of UM patients

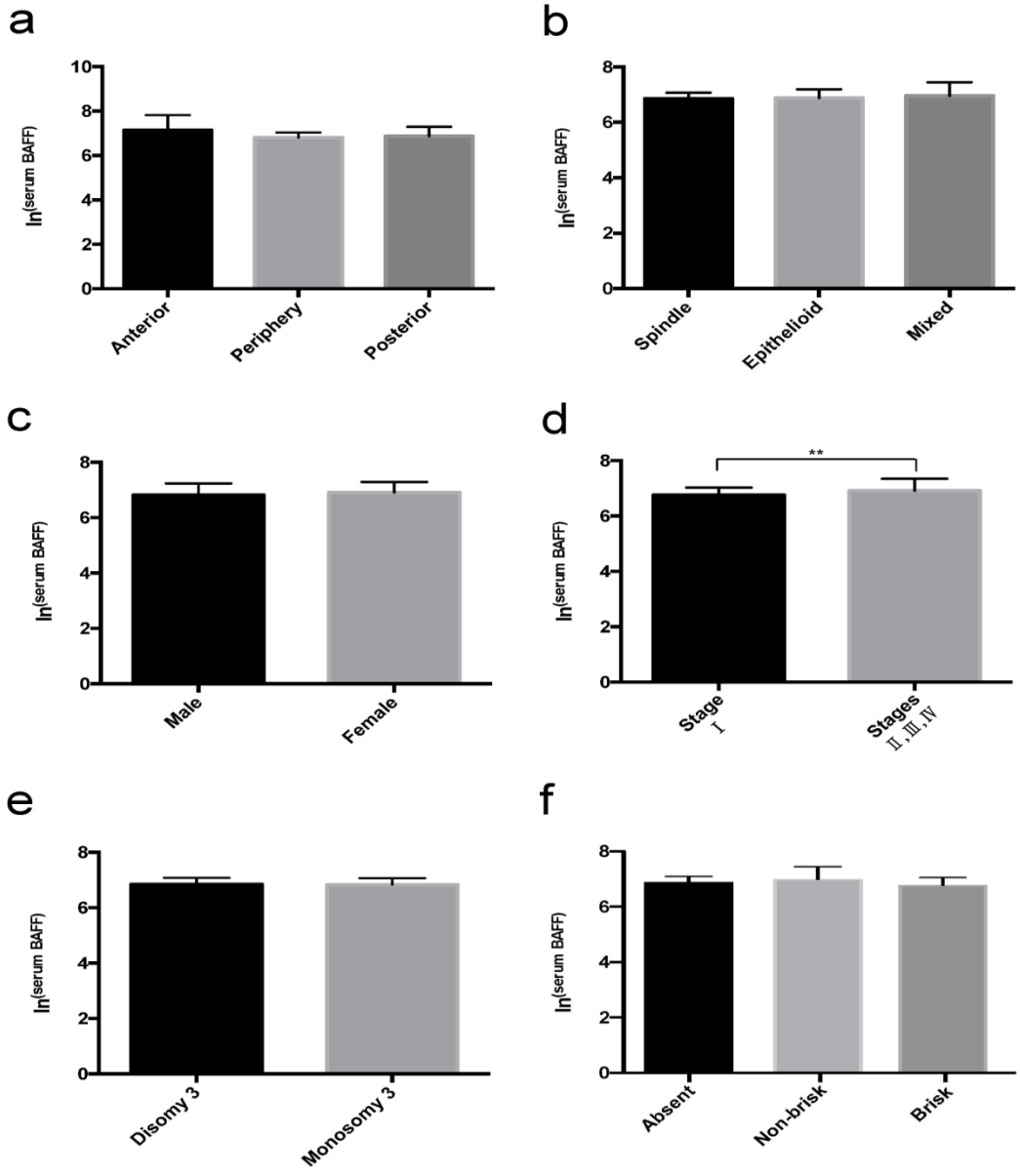


**Figure 7.** (a-f) The comparison of $ln^{(serum\ BAFF)}$ in different tumor locations, histopathological cell types, gender, cancer stages at diagnosis, cytogenetic alterations of chromosome 3 and TILs' categories, respectively.

Note: ** means $P<0.05$.

ANOVA and Tamhane post hoc analysis demonstrated that tumor locations and histopathological cell types had no significant associations with the $\ln^{(\text{serum BAFF})}$.(Lin and Süsskind, 2020) (see Figure 7.a-b) While serum BAFF concentrations were confirmed to be independent of gender, cytogenetic alterations of chromosome 3 and TILs' categories, the patients in the advanced cancer stages (II, III and IV) were identified to have significantly higher $\ln^{(\text{serum BAFF})}$ than those in the early-stage I.(Lin and Süsskind, 2020) (two-tailed t test, $P<0.05$, see Figure 7.c-f)

## 3.6 Plasma OPN levels and clinicopathological features of UM patients

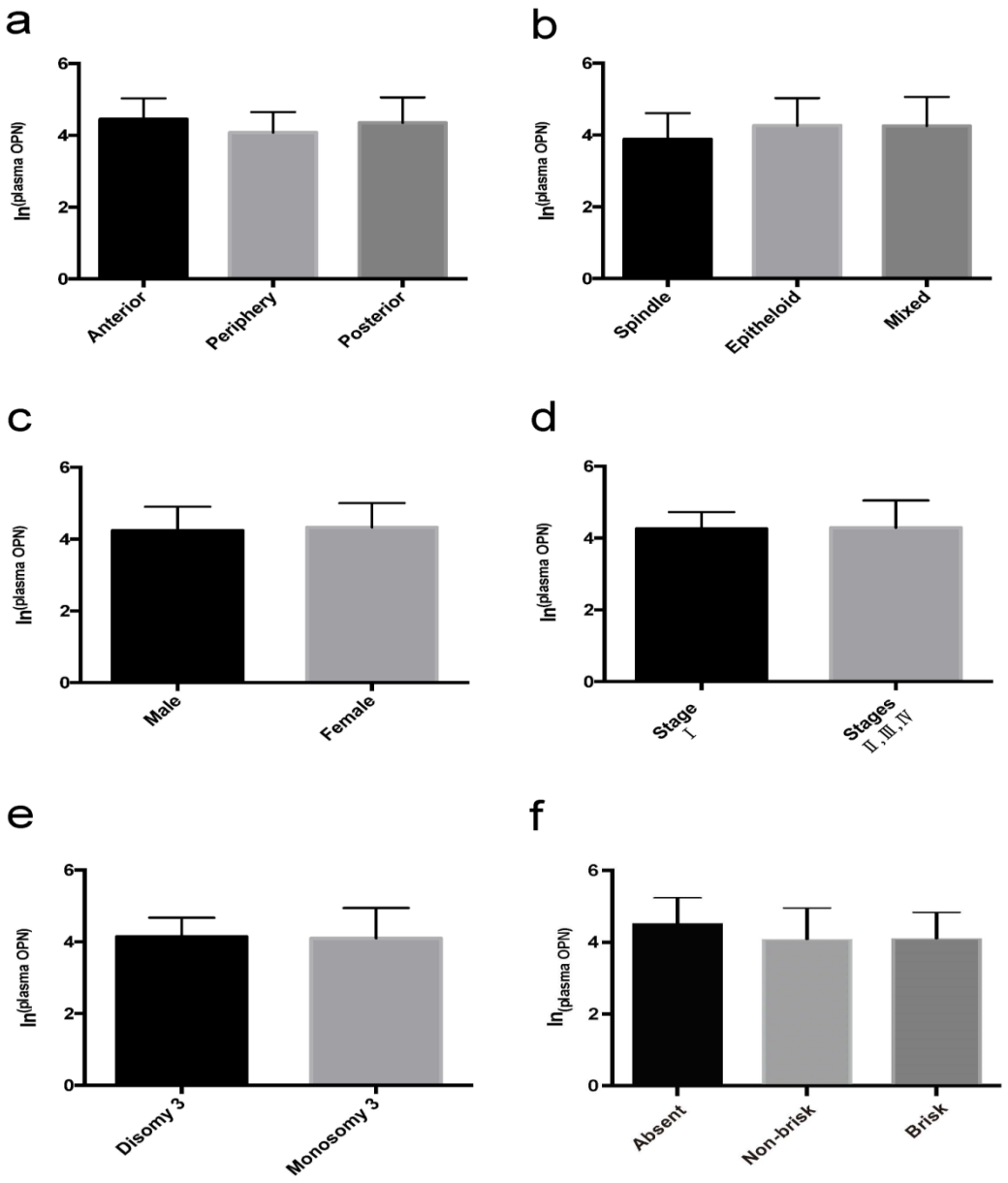


**Figure 8.** (a-f) The comparison of $ln^{(plasma\ OPN)}$ in different tumor lesions, histopathological types, gender, cancer stages at diagnosis, cytogenetic alterations of chromosome 3 and TILs' categories, respectively.

Statistical analysis did not show significant differences in the plasma OPN levels with respect to diverse tumor locations, histopathological cell types, gender, cancer stages at diagnosis, cytogenetic alterations of chromosome 3 and TILs' categories. (all $P>0.05$, see Figure 8.a-f)

## 3.7 Serum GDF-15 levels and clinicopathological features of UM patients

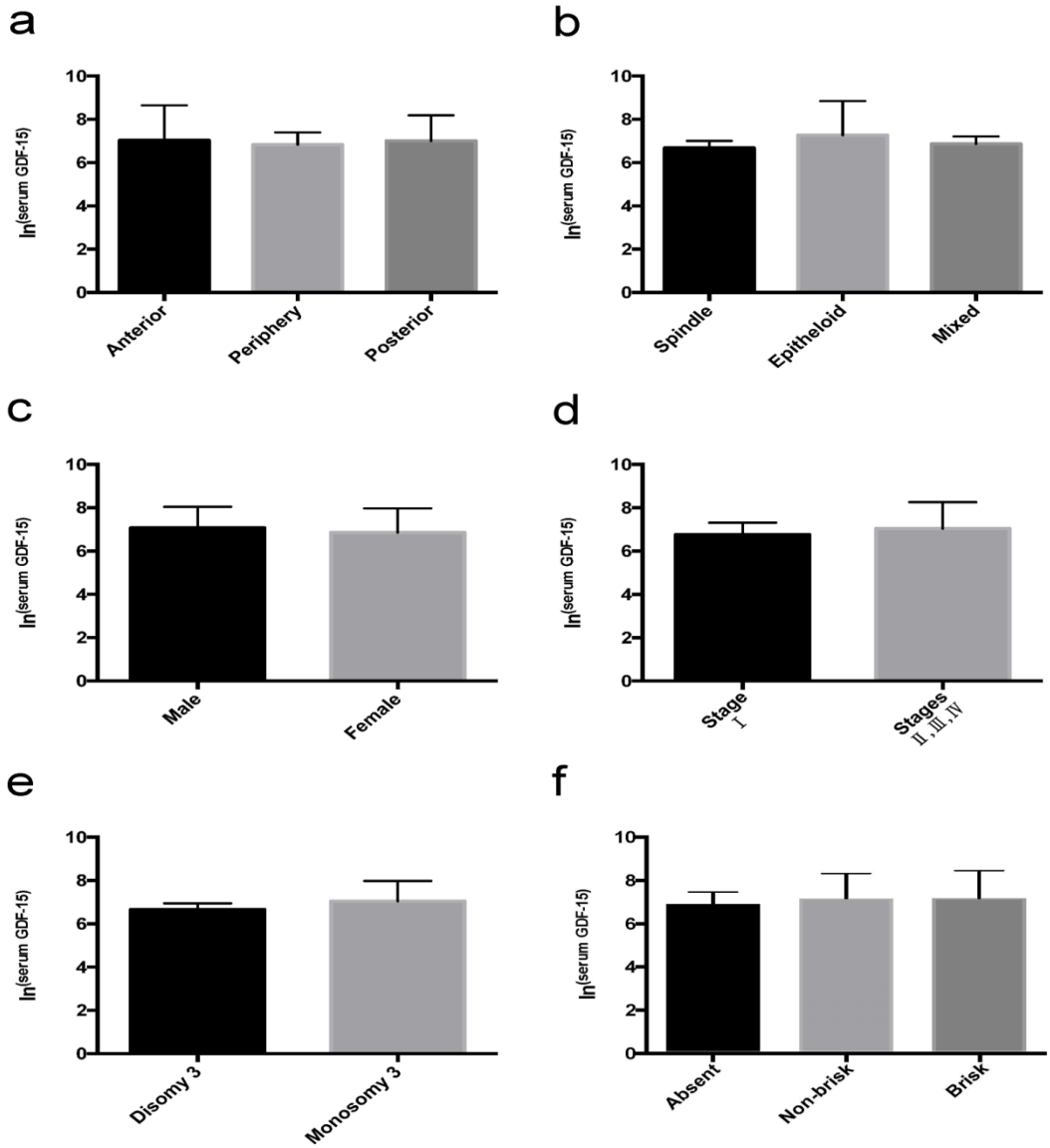

**Figure 9.** (a-f) The comparison of $\ln^{(\text{serum GDF-15})}$ in different tumor lesions, histopathological types, gender, cancer stages at diagnosis, cytogenetic alterations of chromosome 3 and TILs' categories, respectively.

Similar to the plasma OPN, statistical analyses also did not show any significant distinctions in the serum GDF-15 concentrations with respect to different tumor locations, histological cell types, gender, cancer stages, cytogenetic alterations of chromosome 3 and TILs' categories, respectively. (all $P>0.05$, see Figure 9.a-f)

## 3.8 Efficiency of BAFF, OPN and GDF-15 in differentiating patients with early-metastasis from those without

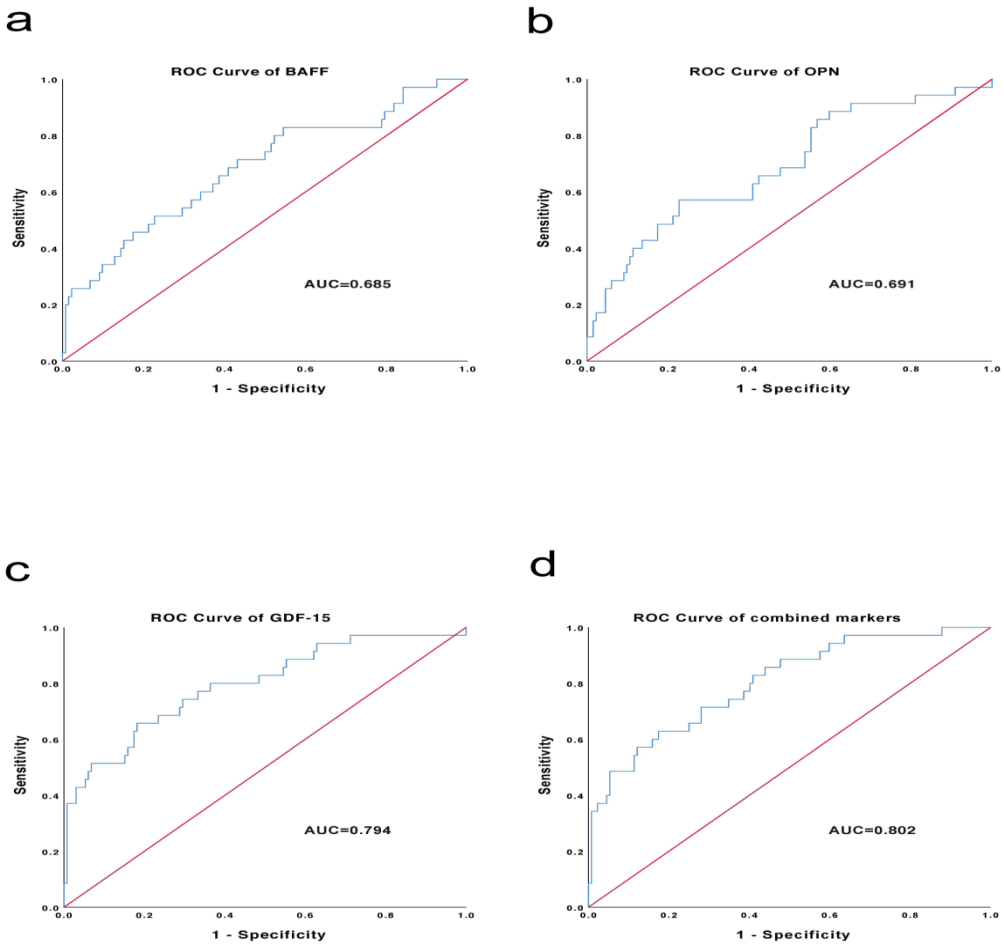

**Figure 10.** (a) Receiver operating characteristic (ROC) curves for the serum BAFF showing an area under curve (AUC) of 0.685; (b) ROC curves for the plasma OPN showing an AUC of 0.691; (c) ROC curves for the serum GDF-15 showing an AUC of 0.794; (d) A combined panel with three biomarkers (BAFF, OPN and GDF-15) showing an AUC of 0.802.

The receiver operating characteristic (ROC) curves were generated to assess the efficiency of BAFF, OPN and GDF-15 in distinguishing the patients with early-metastasis from those without. As shown in Figure 10, GDF-15 had the best performance with an area under curve (AUC) of 0.794 (95% CI, 0.704 to 0.884), followed by OPN with an AUC of 0.691 (95% CI, 0.589 to 0.704) and BAFF with an AUC of 0.685 (95% CI, 0.580 to 0.790). By maximizing the Youden's index, the serum BAFF level of 1120 pg/ml (*J*=0.304, specificity=83.2%, sensitivity=47.2%), the plasma OPN level of 92 ng/ml (*J*=0.363, specificity=76.3%, sensitivity=60.0%) and the serum GDF-15 level of 1209 pg/ml (*J*=0.508, specificity=82.2%, sensitivity=68.6%) were identified to have the best performance for distinguishing the metastatic patients from non-metastatic patients.(Youden, 1950) Of notice, the combination of these three markers offered a better performance than any single biomarker with an AUC of 0.802 (95% confidence interval, 0.718 to 0.885).

Table 4. Application of the cutoff values of three biomarkers in 36 metastatic patients

| Biomarkers | Number of patients |
|---|---|
| Serum BAFF↑ | 16 out of 36 (44.4%) |
| Serum GDF-15↑ | 23 out of 36 (63.9%) |
| Plasma OPN↑ | 20 out of 36 (55.6%) |
| Either serum BAFF↑, or GDF15↑ or plasma OPN↑ | 30 out of 36 (83.3%) |

Note: ↑means that the levels of the corresponding biomarkers are higher than their cutoff values.

Furthermore, the cutoff values of three biomarkers were introduced to briefly assess the first blood samples after diagnosis of metastasis of 36 metastatic patients. (see Table 4.) The results showed that 63.9% of the patients were identified to have enhanced level of

serum GDF-15, while 55.6% and 44.4% of the patients had elevated concentrations of plasma OPN and serum BAFF, respectively. Notably, 83.3% of the patients demonstrated increased expression in at least one of the three biomarkers.

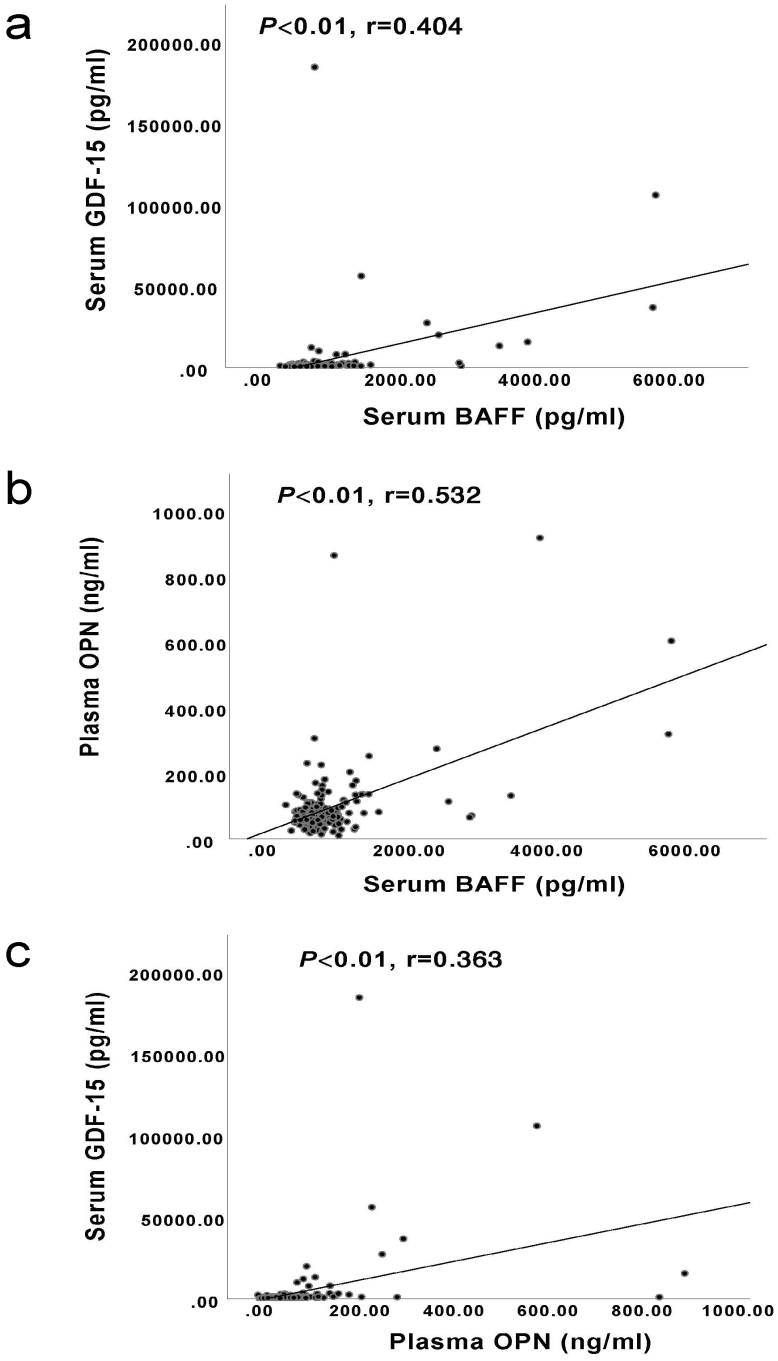

**Figure 11.** (a) The Pearson's correlations between serum BAFF levels and serum GDF-15 levels; (b) The Pearson's correlations between serum BAFF levels and plasma OPN levels; (c) The Pearson's correlations between plasma OPN levels and serum GDF-15 levels.

The Pearson's correlation coefficients were conducted to study these three cytokines. Notably, we observed a moderate correlation between serum BAFF levels and plasma OPN levels. ($P$<0.01, r=0.532, see Figure 11.b) Besides, the statistical analyses on the other two pairs, i.e. serum BAFF and GDF-15 levels ($P$<0.01, r=0.404, see Figure 11.a), plasma OPN and serum GDF-15 levels ($P$<0.01, r=0.363, see Figure 11.c) also revealed significant positive correlations.

## 3.9 Immunohistochemical analysis concerning the expression of BAFF, BAFF-R, TACI, CD3, CD4, CD8 and CD20

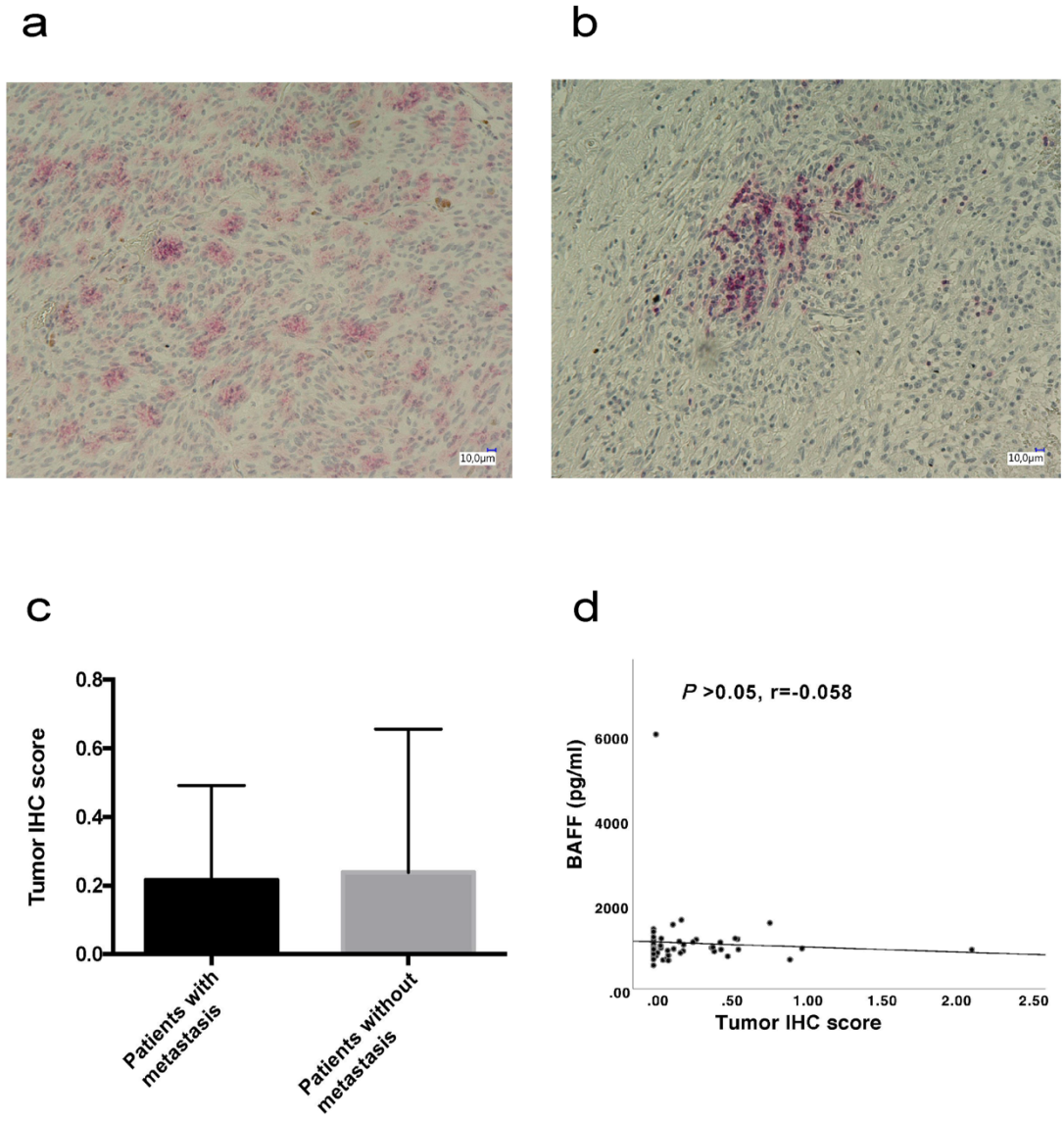


**Figure 12.** (a, b) Photomicrographs showing immunohistochemical staining of BAFF in the cytoplasm of UM tumor cells and lymphocytes, respectively; (c) The comparison of Tumor IHC scores between the patients with metastasis and those without; (d) The Pearson's correlation between serum BAFF levels and Tumor IHC scores.

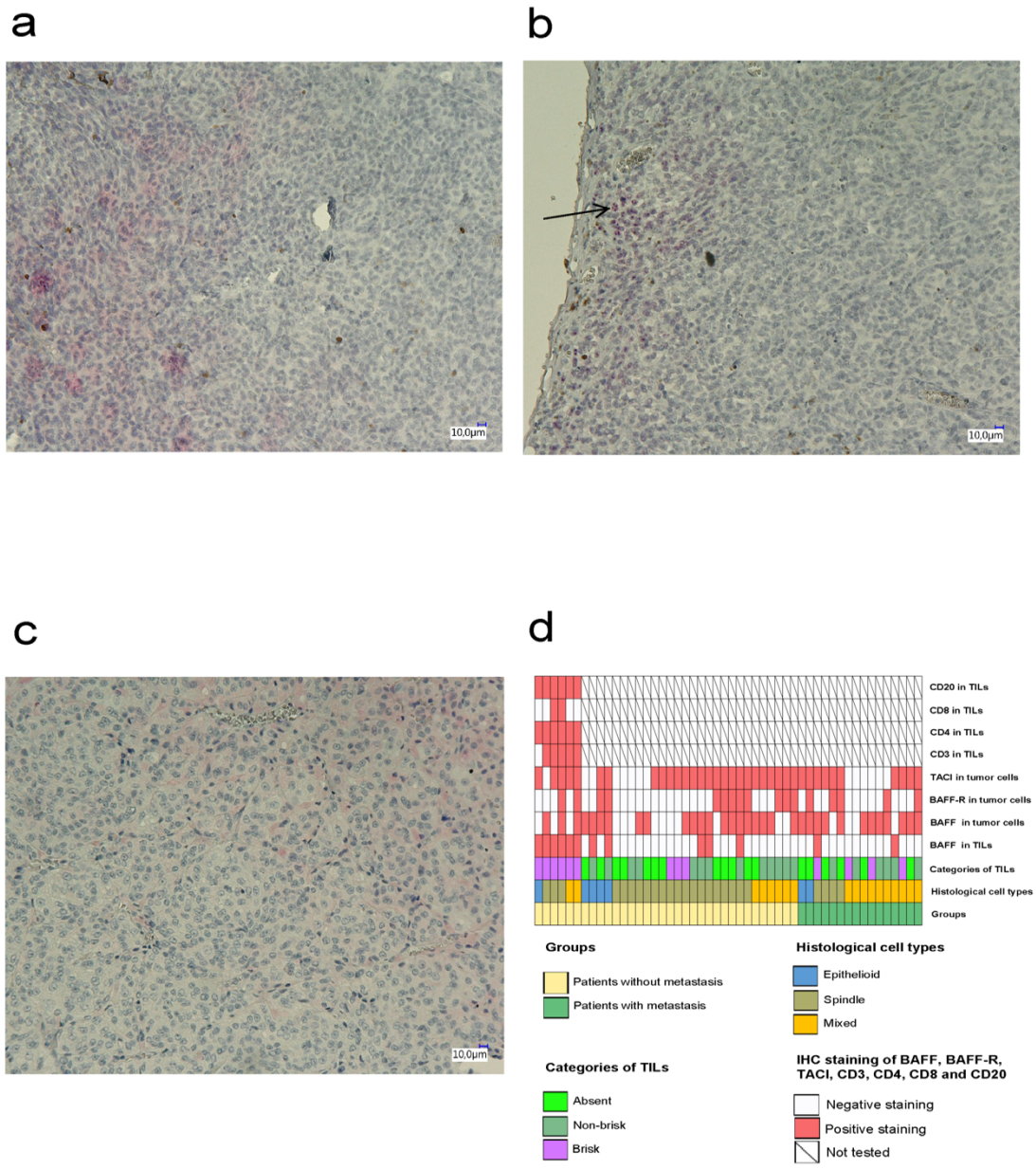


**Figure 13.** (a, b) Photomicrographs showing immunohistochemical staining of BAFF-R in the cytoplasm and nucleus of UM tumor cells, respectively. The tumor cells containing the positive nuclear staining of BAFF-R were majorly located in the marginal area of the tumor (black arrow in Fig 13.b); (c) Photomicrographs showing immunohistochemical staining of TACI in the cytoplasm of UM tumor cells; (d) Heatmap showing the clinicopathological features (metastatic status, histopathological cell types, categories of TILs and the IHC staining results of BAFF, BAFF-R, TACI, CD3, CD4, CD8 and CD20) of 50 UM specimens.

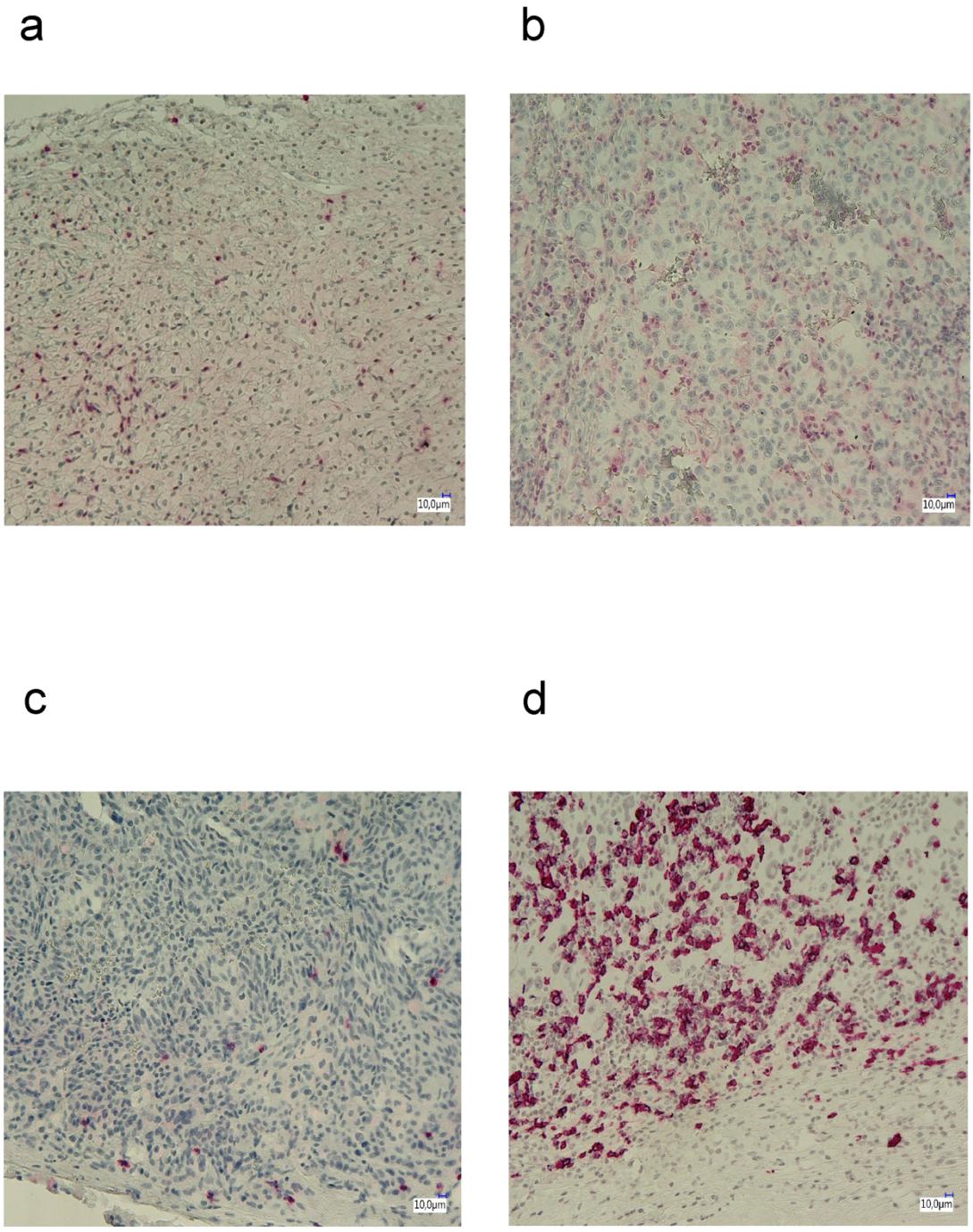


**Figure 14.** (a-d) Photomicrographs showing immunohistochemical staining of CD3, CD4, CD8 and CD20 in the TILs of UM tumor cells, respectively.

50 (16 patients with metastasis and 34 without metastasis) tumor samples were analysed with IHC staining of BAFF.(Lin and Süsskind, 2020) As shown in Figure 12.a and b, BAFF staining was detected in the cytoplasm of the tumor cells and TILs.(Lin and Süsskind, 2020) Among 50 specimens, 17 (34%) did not show BAFF staining in the tumor cells. No significant differences in the Tumor IHC scores were observed between metastatic patients and nonmetastatic patients.(Lin and Süsskind, 2020) (see Figure 12.c, independent samples' t test, two-tailed, $P>0.05$) Additionally, the association between serum BAFF concentrations and the Tumor IHC scores was also evaluated and the results suggested no significant correlation between them.(Lin and Süsskind, 2020) (see Figure 12.d) We also assessed the tumor specimens with respect to two BAFF receptors BAFF-R and TACI. 17 of the 50 specimens (5 from metastatic patients and 12 from non-metastatic patients) demonstrated positive staining of BAFF-R in malignant cells, with 6 presenting in the cytoplasm, 7 in the nucleus and 4 in both locations.(Lin and Süsskind, 2020) (see Figure 13.a-b) Positive staining of TACI was observed in the tumor cells in 36 specimens (10 from metastatic patients and 26 from non-metastatic patients).(Lin and Süsskind, 2020) (see Figure 13.c) Unlike BAFF-R, the staining sites of TACI were all in the cytoplasm.(Lin and Süsskind, 2020) Notably, no lymphocytes showed positive staining of either BAFF-R or TACI in the tested 50 specimens.(Lin and Süsskind, 2020)

We also noticed obvious TILs in 32 of 50 tested specimens.(Lin and Süsskind, 2020) BAFF-positive TILs were found in 13 (6 with brisk category of TILs and 7 with non-brisk category of TILs) of these specimens.(Lin and Süsskind, 2020) (see Figure 12.b and Figure 13.d) Furthermore, the 6 specimens with BAFF-positive brisk category of TILs were further studied according to CD3, CD4, CD8 and CD20 expression. Of notice, all these 6 specimens contained CD4+ and CD20+ TILs, whereas CD3+ and CD8+ TILs were observed only in 5 and 2 specimens, respectively.(Lin and Süsskind, 2020) (see Figure 13.d and Figure 14.a-d)

No obvious differences in the composition of categories of TILs were observed between patients with and those without metastasis.(Lin and Süsskind, 2020) (see Table 3. and Figure 13.d) Besides, no remarkable associations were found between BAFF and its receptors.(Lin and Süsskind, 2020) (see Figure 13.d)

# 4. Discussion

The purpose of our work was to analyse the blood-based biomarkers BAFF, OPN and GDF-15 with respect to detect the early-metastasis of UM patients. To achieve this goal, our preliminary study using a human cytokine array kit with the serum of four UM patients indicated that the patients with metastasis might have significantly higher serum BAFF, GDF-15 and OPN levels than those without. Afterwards, we applied the analysis to 173 UM patients and explored the blood-based expression of these three cytokines. The results confirmed that BAFF, GDF-15 and OPN could be regarded as promising biomarkers for the early-metastases of UM.

## 4.1 The clinicopathological features of enrolled patients

173 UM patients and 23 healthy controls were enrolled into this study. While no remarkable differences in the tumor anatomical locations, age and gender were observed between patients with and without metastasis, the metastatic patients had clearly higher percentages of advanced cancer stages (II, III and IV) at diagnosis, higher percentages of monosomy 3 and larger tumor sizes at diagnosis (i.e. LBD and apical height).(Lin and Süsskind, 2020) (see Table 3.) These results accorded well with prior findings that monosomy 3 and increasing tumor sizes of primary UM were associated with increased risks of metastasis. (Shields et al., 2009, Robertson et al., 2017b) With respect to the histopathological cell types, the patients with metastasis demonstrated obviously higher percentages of mixed cell type (62.5% VS 23.5%) and lower

percentages of spindle cell type (25.0% VS 61.8%) than those without metastasis. Consistently, previous report has confirmed that patients with spindle cell type had higher 5-year survival rate than those with epithelioid and mixed cell types.(Barnhill et al., 2017) Interestingly, their results also suggested a close correlation between mixed cell type and prometastatic angiotropism.(Barnhill et al., 2017)

## 4.2 BAFF and the early-metastasis of UM

We clearly showed that UM patients with clinically overt metastatic diseases had significantly higher serum BAFF levels than non-metastatic patients. So far, no consensus exists concerning the value of serum BAFF concentrations in healthy individuals.(Lin and Süsskind, 2020) In the current work, 23 healthy individuals indicated the normal serum BAFF level to be 810 ± 141 pg/ml (Mean±SD). Comparably, two independent prior observations reported it to be 610±270 pg/ml and 1147±315 pg/ml, respectively.(Koizumi et al., 2013a, Kreuzaler et al., 2012) In this study, we maximized the Youden's index ($J$ =0.304, sensitivity=0.472, specificity=0.832) and found the serum BAFF concentration of 1120 pg/ml to have the best performance for differentiating the patients with metastasis from those without.(Lin and Süsskind, 2020)

We also explored the correlations between serum BAFF levels and several clinicopathological characteristics of UM. The serum BAFF levels were confirmed to be independent of gender and tumor locations. In a multi-omics study on UM, Robertson et al. showed that cytogenetic alterations of chromosome 3 played a critical role in the prognosis of UM patients.(Lin and Süsskind, 2020, Robertson et al., 2017b) UM patients with monosomy 3 were confirmed to have distinctive signaling, genomic and immune profiles which firmly correlated to high metastatic risks and poor outcomes.(Robertson et al., 2017a, Lin and Süsskind, 2020) Nevertheless, in our study, no remarkable difference in the serum BAFF concentrations was observed between patients with monosomy 3 and those with disomy 3.(Robertson et al., 2017a, Lin and

Süsskind, 2020) This suggested that BAFF might be involved in the metastatic process through another mechanism rather than the monosomy 3-associated pathway.(Lin and Süsskind, 2020) Due to the limited amount of cytogenetic data in the current study, further investigations with larger cohorts are still needed to reevaluate these results and demonstrate more robust conclusions. Although the epithelioid cell type was described to be an unfavorable prognostic factor for UM patients, in this work, three histopathological cell types of UM (spindle, epithelioid and mixed types) presented no significant differences in serum BAFF levels between each other.(Kaliki et al., 2015, Lin and Süsskind, 2020) In addition, our results revealed no obvious associations between BAFF expression and the tumor sizes of primary UM (LBD and apical height). Likewise, several previously reported UM-associated biomarkers (e.g. MIA and GDF-15) also indicated no statistically significant correlations with the primary tumor sizes.(Suesskind et al., 2012, Reiniger et al., 2005) Additionally, our work suggested a strong correlation ($P$<0.01, r=0.606, see Figure 6.c) between the serum BAFF levels and metastatic burden.(Lin and Süsskind, 2020) Collectively, the outcomes demonstrated that serum BAFF levels were independent of histomorphological and anatomical properties of the primary tumor, and the upregulated serum BAFF concentrations had a close correlation with the metastatic progression rather than with the course of the primary UM.(Lin and Süsskind, 2020)

In the context of IHC staining of BAFF in UM specimens, we observed no differences between patients with early-metastasis and those without. This outcome may be interpreted as follows.(Lin and Süsskind, 2020) First, the tumor specimens for IHC staining of BAFF were only acquired from less than half of the enrolled patients, thus in this study, the IHC staining might not be sufficient enough to offer a comprehensive and accurate landscape of the BAFF expression for all participating patients.(Lin and Süsskind, 2020) Second, the serum BAFF might be generated and secreted from the primary tumor. Nonetheless, even in one patient, the sera and primary tumor specimens were acquired at different time points which could not match the real status of each

other.(Lin and Süsskind, 2020) Third, serum BAFF might be majorly produced by the metastatic tumors and its expression in the primary lesions could not correctly reflect the blood-based BAFF concentrations.(Lin and Süsskind, 2020) More relevant investigations employing larger cohorts are still needed to validate these findings and supplement the data of metastatic lesions.(Lin and Süsskind, 2020) In addition to the IHC staining in the UM tumor cells, we also noticed in some slides that the TILs were also stained by BAFF. The appearance of immune cells was recognized as positive signals for the prognoses of other malignancies, whereas their presence in UM might imply poor outcomes.(Lin and Süsskind, 2020) This phenomenon was already sporadically reported by prior studies.(Mäkitie et al., 2001, Polak et al., 2007, Robertson et al., 2017a, Bronkhorst et al., 2012, Lin and Süsskind, 2020) Li et al. studied the cutaneous melanoma with single cell sequencing technology and found that the major part of intratumoral proliferating T cells were in a dysfunctional status, failing to execute the successful immune activities against the tumor.(Li et al., 2019, Lin and Süsskind, 2020) Moreover, Triozzi and colleagues also identified the existence of CD8+ regulatory T cells which served to suppress the anti-tumor immune responses and contribute to the progression of UM.(Triozzi et al., 2019, Lin and Süsskind, 2020) In the current work, the lymphocyte staining of BAFF were observed in both of the metastatic patients and non-metastatic patients. (Lin and Süsskind, 2020) However, though the TILs were detected in both of the patients with metastasis and those without, the possibility that their functional states varied from each other could not be excluded.(Lin and Süsskind, 2020) Hence, an in-depth investigation focusing on studying the functional states of TILs in UM should be carried out in future to give a clear scenery of the UM-infiltrating lymphocytes.(Lin and Süsskind, 2020) As its name implied, BAFF (B-cell activating factor), also known as B Lymphocyte Stimulator (BLyS), plays a key role in the immune activities.(Mackay and Schneider, 2009, Lin and Süsskind, 2020) According to prior studies, BAFF was not only functioning to enhance the survival of B cells but also to promote the activities of both CD4+ and

CD8+ T cells. (Mäkitie et al., 2001, Bronkhorst et al., 2012, Lin and Süsskind, 2020) Consistently, our IHC study confirmed the expression of CD3, CD4, CD8 and CD20 in the TILs of UM specimens. Taken together, we think that further comprehensive assessment of the status of UM-infiltrating immune cells is still in imperative need to offer a complete landscape of the tumor microenvironment of UM.(Lin and Süsskind, 2020)

BAFF was also reported to participate in the progression of other cancers such as pancreatic cancer, myeloma, lymphoma and leukemia.(Koizumi et al., 2013b, Pan et al., 2017, Ferrer et al., 2009, Chiu et al., 2007, Pelekanou et al., 2018, Lin and Süsskind, 2020) Besides the immune-related pathways, previous reports also revealed other mechanisms through which BAFF participated in the tumor progression.(Lin and Süsskind, 2020) For example, a study on pancreatic cancer showed that *BAFF* was able to enhance the proliferation and survival of malignant cells through interacting with epithelial mesenchymal transition (EMT)-associated genes like *VIM*, *SNAI1* and *CDH1*.(Koizumi et al., 2013b, Lin and Süsskind, 2020) Furthermore, a breast cancer study done by Pelekanou et al. suggested that *BAFF* would contribute to the stemness of tumor cells by promoting the expression of pluripotency-associated genes e.g. *ALDH1A1*, *KLF4* and *NANOG*. (Pelekanou et al., 2018, Lin and Süsskind, 2020) Since the present work is a pilot study, more UM investigations on elucidating the role of *BAFF* in the abovementioned pathways are still urgently needed.(Lin and Süsskind, 2020)

Fu and colleagues studied the B cells and found that the BAFF-R protein was not only detected in the cytoplasm and plasma membrane but also in the cell nucleus.(Lin and Süsskind, 2020, Fu et al., 2009) They suggested that nuclear BAFF-R could enhance the phosphorylation of histone H3 through IKKβ.(Lin and Süsskind, 2020, Fu et al., 2009) Besides, nuclear BAFF-R was identified to bind the NF-κB and work as a transcriptional cofactor to promote the expression of NF-κB target genes such as *BAFF, CD154*, *CXCL8*, *Bcl-xL*, and *Bfl-1/A1,* which were critical for the survival and

proliferation of B cells.(Fu et al., 2009, Lin and Süsskind, 2020) Herein, we firstly confirmed the presence of BAFF-R in the cytoplasm and nucleus of UM tumor cells.(Lin and Süsskind, 2020) Further studies are still essential to establish whether BAFF-R plays a role in UM tumor cells similar as in B cells.(Lin and Süsskind, 2020) TACI, one of three receptors of BAFF, is majorly found in plasma cells and normal B cells.(Smulski and Eibel, 2018, Lin and Süsskind, 2020) Its expression was also observed in malignancies like thyroid carcinoma and lymphoma.(Moreaux et al., 2009, Lin and Süsskind, 2020) A study on lymphoma showed that the increased expression of TACI inversely correlated with the prognoses of patients.(Moreaux et al., 2009, Lin and Süsskind, 2020) Interestingly, an investigation on chronic lymphocytic leukaemia (CLL) demonstrated that a TACI–immunoglobulin fusion protein could regulate the interaction between BAFF and TACI and then impaired the survival of CLL cells.(Mackay and Browning, 2002, Lin and Süsskind, 2020) Dou and colleagues had studied the non-small cell lung cancer and found that TACI involved in the tumoral progression through the ERK1/2 signaling pathway.(Dou et al., 2016, Lin and Süsskind, 2020) Though we identified the expression of TACI in UM tumor cells, the question that whether it played a role in either carcinogenesis, or progress, or metastasis of the UM still remained open.(Lin and Süsskind, 2020) Besides BAFF, TACI still had two ligands APRIL (A proliferation-inducing ligand) and CAML (Calcium modulating ligand) which were reported to participate in the progression of breast cancer and melanoma.(Long et al., 2013, García-Castro et al., 2015, Lin and Süsskind, 2020) Thus, further in-depth studies on UM were still warranted to offer a more complete interaction network of TACI. As BAFF as well as its two receptors BAFF-R and TACI have been shown in UM cells using IHC, the question is whether UM cells use BAFF in an autocrine signaling way.(Lin and Süsskind, 2020)

## 4.3 OPN and the early-metastasis of UM

As mentioned before, three independent research groups have already indicated the level of blood-based OPN to be a promising biomarker for the early-detection of UM metastasis. (Reiniger et al., 2007, Kadkol et al., 2006, Haritoglou et al., 2009a) According to the study done by Reiniger and colleagues, the median plasma concentration of OPN in healthy individuals was 54.6 ng/ml (ranging from 38.23 to 71.21 ng/ml).(Reiniger et al., 2007) Interestingly, the current study presented very similar results which suggested the plasma OPN levels of healthy controls to be 44.06 ng/ml. We noticed that the same ELISA kit (R&D Systems, Minneapolis, Minnesota, USA) was utilized in the study done by Reiniger et al. and our study. Therefore, we think that the values of plasma OPN identified in the current study could serve as liable reference for further relevant investigations on UM. Nonetheless, we also noticed several studies reporting the levels of plasma OPN which differed greatly from abovementioned investigations. For instance, a study reported a high median concentration of 150 ng/ml (ranging from 25 to 485 ng/ml) in normal individuals.(Wong et al., 2006) Meanwhile, another research group suggested a low median plasma OPN level of 18.0 ng/ml (ranging from 11.3 to 31.5 ng/ml).(Okyay et al., 2011) This large discrepancy in plasma OPN values may be owed to the factors such as the varied amounts of participants of each study, ethnic distinctions among the population and the differences among the ELISA kits. Of notice, Vordermark and colleagues explored the levels of plasma OPN in the patients with head and neck cancer with two different kinds of ELISA kits.(Vordermark et al., 2006) Even measuring the same sample, these two ELISA kits provided distinct plasma OPN levels. These findings showed that the comparison of plasma OPN levels between different studies should be conducted with caution.(Vordermark et al., 2006) Further, the measurement of the plasma OPN expression of UM patients should be conducted with a consistent ELISA system.

In comparison with previous studies on investigating the role of OPN on UM, our work firstly explored the association between OPN and various clinicopathological features. The results indicated the independence of plasma OPN concentrations in the context of patients' clinicopathological parameters such as age, gender, tumor locations, histopathological cell types and monosomy 3. Neither the tumor sizes nor the metastatic burden was found to have significant associations with the plasma OPN levels. Since the limited size of current work may restrict the statistical significance, further studies with a larger cohort were still needed to provide more clear and robust conclusions.

OPN was found to exist in the tumor cells in two forms, i.e. secretory OPN (sOPN) and intracellular/nuclear OPN (iOPN). These two forms were identified to promote the metastasis with pleiotropic roles. Prior studies on malignancies like hepatocellular carcinoma, breast and colorectal cancers revealed that sOPN could initiate the metastasis through enhancing the EMT-related genes such as *TWIST1*, *SNAI1* and *SNAI2* and then decreasing the adhesion of tumor cells.(Kothari et al., 2016, Li et al., 2013, Yu et al., 2018) Moreover, studies on ovarian and breast cancer showed that OPN could promote the expression of HIF-1α in a PI3k/AKT pathway-dependent manner and then regulate *TWIST1* to monitor EMT (epithelial–mesenchymal transition).(Zhao et al., 2018b) By contrary, iOPN was identified to trigger the MET (mesenchymal–epithelial transition) process to induce the metastatic colonization. Intriguingly, VEGF was confirmed to regulate the KDR/PLCγ/PKC pathway to facilitate the translocation of sOPN into iOPN.(Jia et al., 2016)

## 4.4 GDF-15 and the early-metastasis of UM

According to our work, patients with early-metastasis had significantly higher serum GDF-15 levels than those without. We noticed that there is no clear consensus regarding the level of serum GDF-15 in normal individuals. A study done by Wang and

colleagues indicated the value of serum GDF-15 in the healthy population to be 506.2 ± 258.4 pg/ml (Mean±SD) which was close to the value identified in the current work.(Wang et al., 2016b) Nevertheless, other studies reported clearly lower physiological levels of serum GDF-15. (Zhao et al., Zhao et al., 2018a) The variations in the serum GDF-15 levels may also be attributed to factors such as different ELISA kits, different sample sizes and ethnic composition of participated population which were discussed before. Similar to BAFF and OPN, our results also indicated the independence of GDF-15 concentrations in the context of patients' clinicopathological parameters such as age, gender, tumor locations and histopathological cell types. Our study revealed no statistically significant correlation between the serum GDF-15 levels and the metastatic burden. This finding implicates that the serum GDF-15 concentrations may have a close association with the advent of metastasis instead of its courses. Furthermore, we also didn't observe a remarkable distinction in the serum GDF-15 levels between UM patients with monosomy 3 and those with disomy 3. Monosomy 3 was proved to be linked with high metastatic risks and acknowledged as an unfavorable prognostic factor for UM patients.(Robertson et al., 2017b) Basing on the results, we inferred that GDF-15 might participate in the early-metastasis through another mechanism rather than the monosomy 3-related pathway. However, further studies with a larger cohort were still needed to validate these findings.

Previous studies on GDF-15 suggested its divergent roles in the cancer metastasis. On the one hand, it was identified to promote the apoptosis and to suppress the angiogenesis and tumor progression.(Ferrari et al., 2005, Baek et al., 2001) On the other hand, its pro-metastatic function was observed in studies on gastric cancer and cutaneous melanoma.(Ishige et al., 2016, Weide et al., 2016)

Kalli and colleagues had studied pancreatic cancer and found that the GDF-15 expression was upregulated in the metastatic process through the Akt/CREB1 pathway.(Kalli et al., 2019) Other investigations on prostate and colorectal cancer indicated that GDF-15 promoted the metastasis through cooperating with EGR1 or

TGFβ-mediated EMT.(Wang et al., 2019, Li et al., 2015) These pathways should be of value to be analysed in further studies on UM.

The screening of serum GDF-15 levels of UM patients may contribute to the early-detection of metastasis when CT or ultrasonography still showed negative results might increase the resection rate of UM patients and thus enhance the survival.

## 4.5 The performance of multiple panel of BAFF, OPN and GDF-15

As our results indicated, the blood-based levels of BAFF, OPN and GDF-15 were identified to be promising biomarkers for the early-metastasis of UM. The combination of blood-based BAFF, OPN and GDF-15 levels were assessed to determine whether it could provide better performance in the prognosis than using an individual biomarker alone. The combination model had an AUC of 0.802 (95% CI, 0.718 to 0.885) which was larger than any separated single biomarker.

Furthermore, the cutoff values of these three biomarkers were applied to test 36 metastatic UM patients. The results demonstrated that the combination panel had a better performance and identified more metastatic patients than applying GDF-15 solely (83.3% VS 63.9%). (see Table 4.) Defining the optimal tumor-biomarker combination has always been a big challenge for oncological researchers. According to Borrebaeck, the well-characterized combination should be consisted of independent “orthogonal biomarkers” whose information could optimally contribute to the performance of the combination model.(Borrebaeck, 2017a) Interestingly, we observed significant positive correlations among the levels of these three cytokines. (see Figure 11.) Therefore, we estimated that three biomarkers in our work might not be totally independent from each other and they might have some undiscovered associations. More relevant studies should be executed to decipher these results.

## 4.6 Limitations of the study

The interpretation of our results should be carried out with caution due to the following limitations. One major limitation of this study is that only a part of the UM patients went through surgical treatments and thus provided limited amounts of primary tumor specimens for IHC staining and for the analyses of histopathological cell types, copy number variations of chromosome 3 and TILs' categories. Additionally, the lack of data of metastatic lesions is also a disadvantage of this study. The tumor specimens of metastatic diseases would show us whether the explored biomarkers were majorly expressed in either the primary or metastatic tumors or both. Future studies employing data from multiple ophthalmological centers would provide larger cohorts and therefore more robust conclusions.

Despite these limitations, our study confirms that blood-based BAFF, OPN and GDF-15 are promising biomarkers for the early-metastasis of UM. Levels of serum BAFF, GDF-15 and plasma OPN were significantly higher in patients with metastasis than those without. Meanwhile, we noticed that a combination of these three biomarkers will moderately improve the prognostic performance than applying each biomarker solely. In comparison with serum BAFF and plasma OPN, our results indicated serum GDF-15 to be the single most promising candidate biomarker for the early-detection of metastasis of UM. However, given the heterogeneity of UM, some patients only showed increased BAFF or OPN, our work also highlighted the essential for more in-depth studies of UM. Together, we firstly identify BAFF as a serum biomarker for the early metastasis of UM as well as strengthen the evidence base that GDF-15 and OPN were also valid biomarkers with a larger cohort than previous investigations.(Suesskind et al., 2012, Kadkol et al., 2006, Haritoglou et al., 2009b, Reiniger et al., 2007) As the metastasis was a complex process, numerous cytokines were supposed to participate in the procedure.(Steeg, 2016) Thus, further studies are still needed to explore the biomarkers of the early-metastases of UM.

# 5. Summary

## 5.1 Summary

Uveal melanoma (UM) is the most common-seen primary intraocular cancer. Half of the UM patients would develop metastatic diseases which lead to an extremely poor survival rate. The lack of effective therapies for the metastatic UM makes it essential to detect metastasis as early as possible when the surgical interventions still work. The formerly used conventional screening methods for the metastasis were limited by the non-sensitivity, radiation exposure and high expenses. Therefore, a more feasible and efficient approach with cheap cost is still urgently needed. Among a variety of methods, the analysis of the blood-based biomarkers has already been proved to be a useful monitoring tool for the metastases of many tumors. In the current study, we analysed the expression of three blood-based biomarkers BAFF, OPN and GDF-15 and explored their roles in the metastasis of UM. The results indicated BAFF, OPN and GDF-15 to be promising biomarkers for the early-detection of metastasis since the UM patients developing metastasis had significantly higher levels of these three blood-based cytokines than those without metastasis. Moreover, our results also provided their cutoff values for differentiating the patients with early-metastasis. The investigation of the clinicopathological parameters of UM revealed a strong correlation between the serum BAFF levels and metastatic burden. In order to have a deep understanding of the role of BAFF in the UM metastasis, immunohistochemical (IHC) approaches were applied to study the expression of BAFF, its two receptors (BAFF-R and TACI) as well as several critical immune-associated markers in 50 UM tumor specimens. The IHC tests had confirmed the existence of these proteins in the tumor specimens. Since our current

work is a pilot study, in-depth researches employing novel technologies are always warranted to offer more insightful and complete elucidations for the findings described here.

## 5.2 Zusammenfassung

Das Aderhautmelanom (uveales Melanom, UM) ist der häufigste primäre intraokulare maligne Tumor beim Erwachsenen. Ungefähr bei der Hälfte der Patienten treten im Verlauf der Erkrankung Metastasen auf, die zu einer extrem schlechten Überlebensrate führen. Das Fehlen wirksamer Therapien für das metastatische UM macht es erforderlich, die Metastasierung frühzeitig zu erkennen, wenn die chirurgischen Eingriffe noch funktionieren. Die etablierten konventionellen Screening-Methoden für die Metastasierung sind mit einer geringen Sensitivität, einer signifikanten Strahlenexposition und hohen Kosten verbunden. Daher ist nach wie vor dringend ein praktikablerer, effizienterer und kostengünstigerer Ansatz erforderlich. Unter einer Vielzahl von Methoden hat sich die Analyse der blutbasierten Biomarker bereits als nützliches Überwachungswerkzeug für die Metastasen vieler Tumoren erwiesen. In der aktuellen Studie haben wir die Expression von drei blutbasierten Biomarkern BAFF, OPN und GDF-15 analysiert und ihre Rolle bei der Metastasierung des UM untersucht. Die Ergebnisse zeigten, dass BAFF, OPN und GDF-15 vielversprechende Biomarker für die Früherkennung von Metastasen sind, da die UM-Patienten, die Metastasen entwickelten, signifikant höhere Spiegel dieser drei blutbasierten Zytokine aufwiesen als solche ohne Metastasen. Darüber hinaus lieferten unsere Ergebnisse auch ihre Grenzwerte für die Differenzierung der Patienten mit Frühmetastasen. Die Untersuchung der klinisch-pathologischen Parameter des UM ergab eine starke Korrelation zwischen den BAFF-Spiegeln im Serum und der Metastasenlast. Um ein tieferes Verständnis der Rolle von BAFF bei der UM-Metastasierung zu erhalten, wurden immunhistochemische (IHC) Ansätze angewendet, um die Expression von

BAFF, seiner beiden Rezeptoren (BAFF-R und TACI) sowie mehrerer kritischer immunassoziierter Rezeptoren zu untersuchen. Die IHC-Tests an 50 UM-Tumorproben bestätigten die Existenz dieser Proteine in den Tumorproben. Da es sich bei unserer aktuellen Arbeit um eine Pilotstudie handelt, sind eingehende Untersuchungen unter Verwendung neuartiger Technologien immer erforderlich, um die hier beschriebenen Ergebnisse aufschlussreicher und vollständiger zu erläutern.

# 6. List of figures

**Figure 7.** (a-f) The comparison of $\ln^{(\text{serum BAFF})}$ in different tumor locations, histopathological cell types, gender, cancer stages at diagnosis, cytogenetic alterations of chromosome 3 and TILs' categories, respectively.

Note: ** means $P<0.05$.

**Figure 8.** (a-f) The comparison of $\ln^{(\text{plasma OPN})}$ in different tumor lesions, histopathological types, gender, cancer stages at diagnosis, cytogenetic alterations of chromosome 3 and TILs' categories, respectively.

**Figure 9.** (a-f) The comparison of $\ln^{(\text{serum GDF-15})}$ in different tumor lesions, histopathological types, gender, cancer stages at diagnosis, cytogenetic alterations of chromosome 3 and TILs' categories, respectively.

**Figure 10**. (a) Receiver operating characteristic (ROC) curves for the serum BAFF showing an area under curve (AUC) of 0.685; (b) ROC curves for the plasma OPN showing an AUC of 0.691; (c) ROC curves for the serum GDF-15 showing an AUC of 0.794; (d) A combined panel with three biomarkers (BAFF, OPN and GDF-15) showing an AUC of 0.802.

**Figure 11.** (a) The Pearson's correlations between serum BAFF levels and serum GDF-15 levels; (b) The Pearson's correlations between serum BAFF levels and plasma OPN levels; (c) The Pearson's correlations between plasma OPN levels and serum GDF-15 levels.

**Figure 12.** (a, b) Photomicrographs showing immunohistochemical staining of BAFF in the cytoplasm of UM tumor cells and lymphocytes, respectively; (c) The comparison of Tumor IHC scores between the patients with metastasis and those without; (d) The Pearson's correlation between serum BAFF levels and Tumor IHC scores.

**Figure 13.** (a, b) Photomicrographs showing immunohistochemical staining of BAFF-R in the cytoplasm and nucleus of UM tumor cells, respectively. The tumor cells containing the positive nuclear staining of BAFF-R were majorly located in the marginal area of the tumor (black arrow in Fig 13.b); (c) Photomicrographs showing immunohistochemical staining of TACI in the cytoplasm of UM tumor cells; (d) Heatmap showing the clinicopathological features (metastatic status, histopathological cell types,

categories of TILs and the IHC staining results of BAFF, BAFF-R, TACI, CD3, CD4, CD8 and CD20) of 50 UM specimens.

**Figure 14.** (a-d) Photomicrographs showing immunohistochemical staining of CD3, CD4, CD8 and CD20 in the TILs of UM tumor cells, respectively.

# 7. List of tables

# 8. Acknowledgement

The time at Tübingen was a really memorable experience to me. Foremost, I would like to express my greatest thanks to my supervisor Daniela for her kind and sincere help for my doctoral project. I didn't go to deeply into the research of uveal melanoma and had little experience about it before the project started. Her professional guidance and insightful thinking have paved away many obstacles during my study. Moreover, she was always supportive for my extensive studies on new things such as single cell sequencing and whole genome sequencing and offered invaluable suggestions.

I was also lucky to be surrounded by many excellent group members i.e. Ulrike Hagemann, Claudia Riedinger, Heike Enderle and Monika Wild. Their patience in teaching me the detailed process of many experiments has moved me a lot. And their wonderful immunohistochemical staining work contributed greatly to this study.

I would like to thank Dr. You-Shan Feng for the statistical consulting. In the lab, I also met some wonderful students who were at my generation. In particular, I want to thank Wenxu and her husband Fubo. Their optimismus and diligence always inspires me a lot. Outside the lab, they also showed me plenty of things about German society and discussed many interesting topics with me. They not only give invaluable views for my study but also great assistance in integration into my studying life in Germany.

I would also like to thank the China Scholarship Council (CSC) for their financial support for my doctoral study and living in Tübingen.

Last but not the least, I want to thank my wife, my parents and my grandmother. Without their unconditional love and support, I would not come to Tübingen. I am also grateful to you for the infinite patience in supporting me whenever I am in need of help.

You definitely made a great part of the meaning of my life. It’s fortunate to have you as family members and thanks for everything you have done for me!

To my family, for their unconditional love.

# 9. Erklärung zum Eigenanteil der Dissertationsschrift

Die Arbeit wurde in dem Augenklinik Tübingen unter Betreuung von Prof. Dr. med. Daniela Süsskind durchgeführt.

Die Konzeption der Studie erfolgte in Zusammenarbeit mit Prof. Dr. med. Daniela Süsskind durchgeführt.

Sämtliche Versuche wurden nach Einarbeitung durch Labormitglieder von Prof. Dr. med. Daniela Süsskind und von mir mit Unterstützung durch Prof. Dr. med. Daniela Süsskind durchgeführt.

Die statistische Auswertung erfolgte nach Anleitung durch Prof. Dr. med. Daniela Süsskind und Zenan Lin ducrhgeführt.

Ich versichere, das Manuskript selbständig (nach Anleitung durch Prof. Dr. med. Daniela Süsskind) verfasst zu haben und keine weiteren als die von mir angegebenen Quellen verwendet zu haben.

Tübingen, den

Unterschrift: Lin, Zenan

# 10. Curriculum Vitae

Zenan Lin geb. 08.04.1990 in Fujian, China.

Anschrift: Stäudach 172, 72074 Tübingen, Germany.

**Studium**

University of Tübingen, Tübingen, Germany

Doktor der Medizin. Advisor: Prof. Dr. Daniela Süsskind 2016-2020

Tongji University, Shanghai, China

Master of medicine. Advisor: Prof. Dr. Hongping Cui 2014-2016

Tongji University, Shanghai, China

Bachelor of medicine. 2008-2014

**Ausbildung**

06.2014-09.2016 Praktikum (Augenheilkunde), Shanghai East Hospital

06.2013-06.2014 Praktisches Jahr, Shanghai 10$^{th}$ People's Hospital

**Sprache**

Chinesisch (Muttersprache), Deutsch (TestDaF 16), Englisch (IELTS 7.0)

**Publikationen**

**Lin Z**, Süsskind D. Comparing the prognostic performance of BAFF, GDF-15 and OPN in the early-detection of the metastasis of uveal melanoma. (In preparation)

**Lin Z**, Süsskind D. Exploring the role of BAFF in the early stage of metastasis of uveal melanoma. (Under review)

# 11. References


ABILDGAARD, S. K. O. & VORUM, H. 2013a. Proteomics of Uveal Melanoma: A Minireview. *Journal of Oncology,* 2013**,** 820953.

ABILDGAARD, S. K. O. & VORUM, H. 2013b. Proteomics of uveal melanoma: a minireview. *Journal of oncology,* 2013**,** 820953-820953.

AGUADO, B. A., BUSHNELL, G. G., RAO, S. S., JERUSS, J. S. & SHEA, L. D. 2017. Engineering the pre-metastatic niche. *Nature biomedical engineering,* 1**,** 0077.

AMIN, M. B., EDGE, S., GREENE, F., BYRD, D. R., BROOKLAND, R. K., WASHINGTON, M. K., GERSHENWALD, J. E., COMPTON, C. C., HESS, K. R., SULLIVAN, D. C., JESSUP, J. M., BRIERLEY, J. D., GASPAR, L. E., SCHILSKY, R. L., BALCH, C. M., WINCHESTER, D. P., ASARE, E. A., MADERA, M., GRESS, D. M. & MEYER, L. R. 2017. *AJCC Cancer Staging Manual,* Switzerland, Springer International Publishing.

BAEK, S. J., KIM, K. S., NIXON, J. B., WILSON, L. C. & ELING, T. E. 2001. Cyclooxygenase inhibitors regulate the expression of a TGF-beta superfamily member that has proapoptotic and antitumorigenic activities. *Mol Pharmacol,* 59**,** 901-8.

BAKALIAN, S., MARSHALL, J.-C., LOGAN, P., FAINGOLD, D., MALONEY, S., DI CESARE, S., MARTINS, C., FERNANDES, B. F. & BURNIER, M. N. 2008. Molecular Pathways Mediating Liver Metastasis in Patients with Uveal Melanoma. *Clinical Cancer Research,* 14**,** 951.

BARNHILL, R. L., YE, M., BATISTELLA, A., STERN, M. H., ROMAN-ROMAN, S., DENDALE, R., LANTZ, O., PIPERNO-NEUMANN, S., DESJARDINS, L., CASSOUX, N. & LUGASSY, C. 2017. The biological and prognostic significance of angiotropism in uveal melanoma. *Lab Invest*.

BOOTCOV, M. R., BAUSKIN, A. R., VALENZUELA, S. M., MOORE, A. G., BANSAL, M., HE, X. Y., ZHANG, H. P., DONNELLAN, M., MAHLER, S., PRYOR, K., WALSH, B. J., NICHOLSON, R. C., FAIRLIE, W. D., POR, S. B., ROBBINS, J. M. & BREIT, S. N. 1997. MIC-1, a novel macrophage inhibitory cytokine, is a divergent member of the TGF-beta superfamily. *Proceedings of the National Academy of Sciences of the United States of America,* 94**,** 11514-11519.

BORREBAECK, C. A. 2017a. Precision diagnostics: moving towards protein biomarker signatures of clinical utility in cancer. *Nat Rev Cancer,* 17**,** 199-204.

BORREBAECK, C. A. K. 2017b. Precision diagnostics: moving towards protein biomarker signatures of clinical utility in cancer. *Nature Reviews Cancer,* 17**,** 199.

BOSSERHOFF, A. K., DREAU, D., HEIN, R., LANDTHALER, M., HOLDER, W. D. & BUETTNER, R. 2001. Melanoma inhibitory activity (MIA), a serological marker of malignant melanoma. *Recent Results Cancer Res,* 158**,** 158-68.

BRONKHORST, I. H. G., VU, T. H. K., JORDANOVA, E. S., LUYTEN, G. P. M., BURG, S. H. V. D. & JAGER, M. J. 2012. Different Subsets of Tumor-Infiltrating Lymphocytes Correlate with Macrophage Influx and Monosomy 3 in Uveal MelanomaTumor-Infiltrating

Lymphocytes in Uveal Melanoma. *Investigative Ophthalmology & Visual Science,* 53**,** 5370-5378.

BROWN, J., RATHBONE, E., HINSLEY, S., GREGORY, W., GOSSIEL, F., MARSHALL, H., BURKINSHAW, R., SHULVER, H., THANDAR, H., BERTELLI, G., MACCON, K., BOWMAN, A., HANBY, A., BELL, R., CAMERON, D. & COLEMAN, R. 2018. Associations Between Serum Bone Biomarkers in Early Breast Cancer and Development of Bone Metastasis: Results From the AZURE (BIG01/04) Trial. *JNCI: Journal of the National Cancer Institute,* 110**,** 871-879.

CARVAJAL, R. D., SCHWARTZ, G. K., TEZEL, T., MARR, B., FRANCIS, J. H. & NATHAN, P. D. 2017. Metastatic disease from uveal melanoma: treatment options and future prospects. *The British journal of ophthalmology,* 101**,** 38-44.

CHANDRAN, S. S., SOMERVILLE, R. P. T., YANG, J. C., SHERRY, R. M., KLEBANOFF, C. A., GOFF, S. L., WUNDERLICH, J. R., DANFORTH, D. N., ZLOTT, D., PARIA, B. C., SABESAN, A. C., SRIVASTAVA, A. K., XI, L., PHAM, T. H., RAFFELD, M., WHITE, D. E., TOOMEY, M. A., ROSENBERG, S. A. & KAMMULA, U. S. 2017. Treatment of metastatic uveal melanoma with adoptive transfer of tumour-infiltrating lymphocytes: a single-centre, two-stage, single-arm, phase 2 study. *Lancet Oncol,* 18**,** 792-802.

CHATTOPADHYAY, C., KIM, D. W., GOMBOS, D. S., OBA, J., QIN, Y., WILLIAMS, M. D., ESMAELI, B., GRIMM, E. A., WARGO, J. A., WOODMAN, S. E. & PATEL, S. P. 2016. Uveal melanoma: From diagnosis to treatment and the science in between. *Cancer,* 122**,** 2299-2312.

CHERECHES, G., BARBOS, O., BUIGA, R., BALACESCU, O., IANCU, D., TODOR, N., BALACESCU, L., MIRON, N., BEJINARIU, N. & CIULEANU, T.-E. J. J. O. B. O. O. J. O. T. B. U. O. O. 2017. Biomarkers for the early detection of relapses in metastatic colorectal cancers. *J BUON,* 22**,** 658-666.

CHIU, A., XU, W., HE, B., DILLON, S. R., GROSS, J. A., SIEVERS, E., QIAO, X., SANTINI, P., HYJEK, E., LEE, J. W., CESARMAN, E., CHADBURN, A., KNOWLES, D. M. & CERUTTI, A. 2007. Hodgkin lymphoma cells express TACI and BCMA receptors and generate survival and proliferation signals in response to BAFF and APRIL. *Blood,* 109**,** 729-39.

CLARK JR, W. H., ELDER, D. E., GUERRY IV, D., BRAITMAN, L. E., TROCK, B. J., SCHULTZ, D., SYNNESTVEDT, M. & HALPERN, A. C. 1989. Model predicting survival in stage I melanoma based on tumor progression. *JNCI: Journal of the National Cancer Institute,* 81**,** 1893-1904.

CRISTAUDO, A., FODDIS, R., BONOTTI, A., SIMONINI, S., VIVALDI, A., GUGLIELMI, G., AMBROSINO, N., CANESSA, P. A., CHELLA, A., LUCCHI, M., MUSSI, A. & MUTTI, L. 2010. Comparison between plasma and serum osteopontin levels: usefulness in diagnosis of epithelial malignant pleural mesothelioma. *The International journal of biological markers,* 25**,** 164-170.

DIENER-WEST, M., REYNOLDS, S. M., AGUGLIARO, D. J., CALDWELL, R., CUMMING, K., EARLE, J. D., GREEN, D. L., HAWKINS, B. S., HAYMAN, J., JAIYESIMI, I., KIRKWOOD, J. M., KOH, W.-J., ROBERTSON, D. M., SHAW, J. M., THOMA, J. & COLLABORATIVE OCULAR MELANOMA STUDY GROUP, R. 2004. Screening for

metastasis from choroidal melanoma: the Collaborative Ocular Melanoma Study Group Report 23. *Journal of clinical oncology : official journal of the American Society of Clinical Oncology,* 22**,** 2438-2444.

DOU, H., YAN, Z., ZHANG, M. & XU, X. 2016. APRIL, BCMA and TACI proteins are abnormally expressed in non-small cell lung cancer. *Oncol Lett,* 12**,** 3351-3355.

EMMERSON, P. J., DUFFIN, K. L., CHINTHARLAPALLI, S. & WU, X. 2018. GDF15 and Growth Control. *Frontiers in Physiology,* 9**,** 1712.

ESKELIN, S., PYRHÖNEN, S., SUMMANEN, P., PRAUSE, J. U. & KIVELÄ, T. 1999. Screening for metastatic malignant melanoma of the uvea revisited. *Cancer,* 85**,** 1151-9.

FERRARI, N., PFEFFER, U., DELL'EVA, R., AMBROSINI, C., NOONAN, D. M. & ALBINI, A. 2005. The transforming growth factor-beta family members bone morphogenetic protein-2 and macrophage inhibitory cytokine-1 as mediators of the antiangiogenic activity of N-(4-hydroxyphenyl)retinamide. *Clin Cancer Res,* 11**,** 4610-9.

FERRER, G., HODGSON, K. E., ABRISQUETA, P., PONS, A., JANSA, S., GEL, B., FILELLA, X., COLOMER, D., PEREIRA, A., MONTSERRAT, E. & MORENO, C. 2009. BAFF and APRIL in Chronic Lymphocytic Leukemia: Clinico-Biological Correlates and Prognostic Significance. *Blood,* 114**,** 1235.

FIELD, M. G., DECATUR, C. L., KURTENBACH, S., GEZGIN, G., VAN DER VELDEN, P. A., JAGER, M. J., KOZAK, K. N. & HARBOUR, J. W. 2016. PRAME as an Independent Biomarker for Metastasis in Uveal Melanoma. *Clin Cancer Res,* 22**,** 1234-42.

FRY, S. A., ROBERTSON, C. E., SWANN, R. & DWEK, M. V. 2016. Cadherin-5: a biomarker for metastatic breast cancer with optimum efficacy in oestrogen receptor-positive breast cancers with vascular invasion. *British Journal of Cancer,* 114**,** 1019-1026.

FU, L., LIN-LEE, Y. C., PHAM, L. V., TAMAYO, A. T., YOSHIMURA, L. C. & FORD, R. J. 2009. BAFF-R promotes cell proliferation and survival through interaction with IKKbeta and NF-kappaB/c-Rel in the nucleus of normal and neoplastic B-lymphoid cells. *Blood,* 113**,** 4627-36.

GARCÍA-CASTRO, A., ZONCA, M., FLORINDO-PINHEIRO, D., CARVALHO-PINTO, C. E., CORDERO, A., GUTIÉRREZ DEL FERNANDO, B., GARCÍA-GRANDE, A., MAÑES, S., HAHNE, M., GONZÁLEZ-SUÁREZ, E. & PLANELLES, L. 2015. APRIL promotes breast tumor growth and metastasis and is associated with aggressive basal breast cancer. *Carcinogenesis,* 36**,** 574-84.

HANASH, S. M., BAIK, C. S. & KALLIONIEMI, O. 2011. Emerging molecular biomarkers--blood-based strategies to detect and monitor cancer. *Nat Rev Clin Oncol,* 8**,** 142-50.

HARITOGLOU, I., WOLF, A., MAIER, T., HARITOGLOU, C., HEIN, R. & SCHALLER, U. C. 2009a. Osteopontin and 'melanoma inhibitory activity': comparison of two serological tumor markers in metastatic uveal melanoma patients. *Ophthalmologica,* 223**,** 239-43.

HARITOGLOU, I., WOLF, A., MAIER, T., HARITOGLOU, C., HEIN, R. & SCHALLER, U. C. 2009b. Osteopontin and 'Melanoma Inhibitory Activity': Comparison of Two Serological Tumor Markers in Metastatic Uveal Melanoma Patients. *Ophthalmologica,* 223**,** 239-243.

HICKS, C., FOSS, A. J. & HUNGERFORD, J. L. 1998. Predictive power of screening tests for metastasis in uveal melanoma. *Eye (Lond),* 12 ( Pt 6)**,** 945-8.

ISHIGE, T., NISHIMURA, M., SATOH, M., FUJIMOTO, M., FUKUYO, M., SEMBA, T., KADO, S., TSUCHIDA, S., SAWAI, S., MATSUSHITA, K., TOGAWA, A., MATSUBARA, H., KANEDA, A. & NOMURA, F. 2016. Combined Secretomics and Transcriptomics Revealed Cancer-Derived GDF15 is Involved in Diffuse-Type Gastric Cancer Progression and Fibroblast Activation. *Scientific Reports,* 6**,** 21681.

JIA, R., LIANG, Y., CHEN, R., LIU, G., WANG, H., TANG, M., ZHOU, X., WANG, H., YANG, Y., WEI, H., LI, B., SONG, Y. & ZHAO, J. 2016. Osteopontin facilitates tumor metastasis by regulating epithelial–mesenchymal plasticity. *Cell Death & Disease,* 7**,** e2564-e2564.

KADKOL, S. S., LIN, A. Y., BARAK, V., KALICKMAN, I., LEACH, L., VALYI-NAGY, K., MAJUMDAR, D., SETTY, S., MANIOTIS, A. J., FOLBERG, R. & PE'ER, J. 2006. Osteopontin Expression and Serum Levels in Metastatic Uveal Melanoma: A Pilot Study. *Investigative Ophthalmology & Visual Science,* 47**,** 802-806.

KALIKI, S., SHIELDS, C. L. & SHIELDS, J. A. 2015. Uveal melanoma: estimating prognosis. *Indian journal of ophthalmology,* 63**,** 93-102.

KALLI, M., MINIA, A., PLIAKA, V., FOTIS, C., ALEXOPOULOS, L. G. & STYLIANOPOULOS, T. 2019. Solid stress-induced migration is mediated by GDF15 through Akt pathway activation in pancreatic cancer cells. *Scientific Reports,* 9**,** 978.

KOIZUMI, M., HIASA, Y., KUMAGI, T., YAMANISHI, H., AZEMOTO, N., KOBATA, T., MATSUURA, B., ABE, M. & ONJI, M. 2013a. Increased B Cell-Activating Factor Promotes Tumor Invasion and Metastasis in Human Pancreatic Cancer. *PLOS ONE,* 8**,** e71367.

KOIZUMI, M., HIASA, Y., KUMAGI, T., YAMANISHI, H., AZEMOTO, N., KOBATA, T., MATSUURA, B., ABE, M. & ONJI, M. J. P. O. 2013b. Increased B cell-activating factor promotes tumor invasion and metastasis in human pancreatic cancer. 8**,** e71367.

KOTHARI, A. N., ARFFA, M. L., CHANG, V., BLACKWELL, R. H., SYN, W. K., ZHANG, J., MI, Z. & KUO, P. C. 2016. Osteopontin-A Master Regulator of Epithelial-Mesenchymal Transition. *J Clin Med,* 5.

KRANTZ, B. A., DAVE, N., KOMATSUBARA, K. M., MARR, B. P. & CARVAJAL, R. D. 2017. Uveal melanoma: epidemiology, etiology, and treatment of primary disease. *Clinical ophthalmology (Auckland, N.Z.),* 11**,** 279-289.

KREUZALER, M., RAUCH, M., SALZER, U., BIRMELIN, J., RIZZI, M., GRIMBACHER, B., PLEBANI, A., LOUGARIS, V., QUINTI, I., THON, V., LITZMAN, J., SCHLESIER, M., WARNATZ, K., THIEL, J., ROLINK, A. G. & EIBEL, H. 2012. Soluble BAFF Levels Inversely Correlate with Peripheral B Cell Numbers and the Expression of BAFF Receptors. *The Journal of Immunology,* 188**,** 497.

LI, C., WANG, J., KONG, J., TANG, J., WU, Y., XU, E., ZHANG, H. & LAI, M. 2015. GDF15 promotes EMT and metastasis in colorectal cancer. *Oncotarget; Vol 7, No 1*.

LI, C., WANG, J., KONG, J., TANG, J., WU, Y., XU, E., ZHANG, H. & LAI, M. 2016. GDF15 promotes EMT and metastasis in colorectal cancer. *Oncotarget,* 7**,** 860-872.

LI, H., VAN DER LEUN, A. M., YOFE, I., LUBLING, Y., GELBARD-SOLODKIN, D., VAN AKKOOI, A. C. J., VAN DEN BRABER, M., ROZEMAN, E. A., HAANEN, J. B. A. G., BLANK, C. U., HORLINGS, H. M., DAVID, E., BARAN, Y., BERCOVICH, A., LIFSHITZ, A., SCHUMACHER, T. N., TANAY, A. & AMIT, I. 2019. Dysfunctional CD8 T Cells Form

a Proliferative, Dynamically Regulated Compartment within Human Melanoma. *Cell,* 176**,** 775-789.e18.

LI, N. Y., WEBER, C. E., MI, Z., WAI, P. Y., CUEVAS, B. D. & KUO, P. C. 2013. Osteopontin up-regulates critical epithelial-mesenchymal transition transcription factors to induce an aggressive breast cancer phenotype. *J Am Coll Surg,* 217**,** 17-26; discussion 26.

LIED, G. A. & BERSTAD, A. 2011. Functional and clinical aspects of the B-cell-activating factor (BAFF): a narrative review. *Scand J Immunol,* 73**,** 1-7.

LIN, Z. & SÜSSKIND, D. 2020. Exploring the role of BAFF in the early stage of metastasis of uveal melanoma. *(In submission)*.

LIOTTA, L. A., FERRARI, M. & PETRICOIN, E. 2003. Clinical proteomics: written in blood. *Nature,* 425**,** 905.

LONG, T., SU, J., TANG, W., LUO, Z., LIU, S., LIU, Z., ZHOU, H., QI, M., ZENG, W., ZHANG, J. & CHEN, X. 2013. A novel interaction between calcium-modulating cyclophilin ligand and Basigin regulates calcium signaling and matrix metalloproteinase activities in human melanoma cells. *Cancer Lett,* 339**,** 93-101.

MACKAY, F. & BROWNING, J. L. 2002. BAFF: a fundamental survival factor for B cells. *Nat Rev Immunol,* 2**,** 465-75.

MACKAY, F. & SCHNEIDER, P. 2009. Cracking the BAFF code. *Nature Reviews Immunology,* 9**,** 491-502.

MÄKITIE, T., SUMMANEN, P., TARKKANEN, A. & KIVELÄ, T. 2001. Tumor-Infiltrating Macrophages (CD68+ Cells) and Prognosis in Malignant Uveal Melanoma. *Investigative Ophthalmology & Visual Science,* 42**,** 1414-1421.

MOREAUX, J., VEYRUNE, J. L., DE VOS, J. & KLEIN, B. 2009. APRIL is overexpressed in cancer: link with tumor progression. *BMC Cancer,* 9**,** 83.

MOURIAUX, F., DIORIO, C., BERGERON, D., BERCHI, C. & ROUSSEAU, A. 2012. Liver function testing is not helpful for early diagnosis of metastatic uveal melanoma. *Ophthalmology,* 119**,** 1590-5.

OKYAY, K., TAVIL, Y., SAHINARSLAN, A., TACOY, G., TURFAN, M., SEN, N., GURBAHAR, O., BOYACI, B., YALCIN, R., DEMIRKAN, D. & CENGEL, A. 2011. Plasma osteopontin levels in prediction of prognosis in acute myocardial infarction. *Acta Cardiologica,* 66**,** 197-202.

PAN, J., SUN, Y., ZHANG, N., LI, J., TA, F., WEI, W., YU, S. & AI, L. 2017. Characteristics of BAFF and APRIL factor expression in multiple myeloma and clinical significance. *Oncol Lett,* 14**,** 2657-2662.

PELEKANOU, V., NOTAS, G., ATHANASOULI, P., ALEXAKIS, K., KIAGIADAKI, F., PEROULIS, N., KALYVIANAKI, K., KAMPOURI, E., POLIOUDAKI, H., THEODOROPOULOS, P., TSAPIS, A., CASTANAS, E. & KAMPA, M. 2018. BCMA (TNFRSF17) Induces APRIL and BAFF Mediated Breast Cancer Cell Stemness. *Frontiers in Oncology,* 8**,** 301.

PIPERNO-NEUMANN, S., PIULATS, M. J., GOEBELER, M., GALLOWAY, I., LUGOWSKA, I., BECKER, C. J., VIHINEN, P., VAN CALSTER, J., HADJISTILIANOU, T., PROENÇA, R., CAMINAL, M. J., ROGASIK, M., BLAY, J.-Y. & KAPITEIJN, E. 2019. Uveal Melanoma: A European Network to Face the Many Challenges of a Rare Cancer. *Cancers,* 11.

POLAK, M. E., BORTHWICK, N. J., JOHNSON, P., HUNGERFORD, J. L., HIGGINS, B., DI PALMA, S., JAGER, M. J. & CREE, I. A. 2007. Presence and phenotype of dendritic cells in uveal melanoma. *The British journal of ophthalmology,* 91**,** 971-976.

POUDINEH, M., SARGENT, E. H., PANTEL, K. & KELLEY, S. O. 2018. Profiling circulating tumour cells and other biomarkers of invasive cancers. *Nature Biomedical Engineering,* 2**,** 72-84.

RANGASWAMI, H., BULBULE, A. & KUNDU, G. C. 2006. Osteopontin: role in cell signaling and cancer progression. *Trends Cell Biol,* 16**,** 79-87.

REINIGER, I. W., SCHALLER, U. C., HARITOGLOU, C., HEIN, R., BOSSERHOFF, A. K., KAMPIK, A. & MUELLER, A. J. 2005. "Melanoma inhibitory activity" (MIA): a promising serological tumour marker in metastatic uveal melanoma. *Graefe's Archive for Clinical and Experimental Ophthalmology,* 243**,** 1161-1166.

REINIGER, I. W., WOLF, A., WELGE-LÜSSEN, U., MUELLER, A. J., KAMPIK, A. & SCHALLER, U. C. 2007. Osteopontin as a Serologic Marker for Metastatic Uveal Melanoma: Results of a Pilot Study. *American Journal of Ophthalmology,* 143**,** 705-707.

RIZZARDI, A. E., JOHNSON, A. T., VOGEL, R. I., PAMBUCCIAN, S. E., HENRIKSEN, J., SKUBITZ, A. P., METZGER, G. J. & SCHMECHEL, S. C. 2012. Quantitative comparison of immunohistochemical staining measured by digital image analysis versus pathologist visual scoring. *Diagnostic pathology,* 7**,** 42-42.

ROBERTSON, A. G., SHIH, J., YAU, C., GIBB, E. A., OBA, J., MUNGALL, K. L., HESS, J. M., UZUNANGELOV, V., WALTER, V., DANILOVA, L., LICHTENBERG, T. M., KUCHERLAPATI, M., KIMES, P. K., TANG, M., PENSON, A., BABUR, O., AKBANI, R., BRISTOW, C. A., HOADLEY, K. A., IYPE, L., CHANG, M. T., ABDEL-RAHMAN, M. H., AKBANI, R., ALLY, A., AUMAN, J. T., BABUR, O., BALASUNDARAM, M., BALU, S., BENZ, C., BEROUKHIM, R., BIROL, I., BODENHEIMER, T., BOWEN, J., BOWLBY, R., BRISTOW, C. A., BROOKS, D., CARLSEN, R., CEBULLA, C. M., CHANG, M. T., CHERNIACK, A. D., CHIN, L., CHO, J., CHUAH, E., CHUDAMANI, S., CIBULSKIS, C., CIBULSKIS, K., COPE, L., COUPLAND, S. E., DANILOVA, L., DEFREITAS, T., DEMCHOK, J. A., DESJARDINS, L., DHALLA, N., ESMAELI, B., FELAU, I., FERGUSON, M. L., FRAZER, S., GABRIEL, S. B., GASTIER-FOSTER, J. M., GEHLENBORG, N., GERKEN, M., GERSHENWALD, J. E., GETZ, G., GIBB, E. A., GRIEWANK, K. G., GRIMM, E. A., HAYES, D. N., HEGDE, A. M., HEIMAN, D. I., HELSEL, C., HESS, J. M., HOADLEY, K. A., HOBENSACK, S., HOLT, R. A., HOYLE, A. P., HU, X., HUTTER, C. M., JAGER, M. J., JEFFERYS, S. R., JONES, C. D., JONES, S. J. M., KANDOTH, C., KASAIAN, K., KIM, J., KIMES, P. K., KUCHERLAPATI, M., KUCHERLAPATI, R., LANDER, E., LAWRENCE, M. S., LAZAR, A. J., LEE, S., LERAAS, K. M., LICHTENBERG, T. M., LIN, P., LIU, J., LIU, W., LOLLA, L., LU, Y., IYPE, L., MA, Y., et al. 2017a. Integrative Analysis Identifies Four Molecular and Clinical Subsets in Uveal Melanoma. *Cancer Cell,* 32**,** 204-220.e15.

ROBERTSON, A. G., SHIH, J., YAU, C., GIBB, E. A., OBA, J., MUNGALL, K. L., HESS, J. M., UZUNANGELOV, V., WALTER, V., DANILOVA, L., LICHTENBERG, T. M., KUCHERLAPATI, M., KIMES, P. K., TANG, M., PENSON, A., BABUR, O., AKBANI, R., BRISTOW, C. A., HOADLEY, K. A., IYPE, L., CHANG, M. T., CHERNIACK, A. D., BENZ,

C., MILLS, G. B., VERHAAK, R. G. W., GRIEWANK, K. G., FELAU, I., ZENKLUSEN, J. C., GERSHENWALD, J. E., SCHOENFIELD, L., LAZAR, A. J., ABDEL-RAHMAN, M. H., ROMAN-ROMAN, S., STERN, M. H., CEBULLA, C. M., WILLIAMS, M. D., JAGER, M. J., COUPLAND, S. E., ESMAELI, B., KANDOTH, C. & WOODMAN, S. E. 2017b. Integrative Analysis Identifies Four Molecular and Clinical Subsets in Uveal Melanoma. *Cancer Cell,* 32**,** 204-220.e15.

SHAO, Y., YU, Y., HE, Y., CHEN, Q. & LIU, H. 2019. Serum ATX as a novel biomarker for breast cancer. *Medicine,* 98.

SHIELDS, C. L., FURUTA, M., THANGAPPAN, A., NAGORI, S., MASHAYEKHI, A., LALLY, D. R., KELLY, C. C., RUDICH, D. S., NAGORI, A. V., WAKADE, O. A., MEHTA, S., FORTE, L., LONG, A., DELLACAVA, E. F., KAPLAN, B. & SHIELDS, J. A. 2009. Metastasis of Uveal Melanoma Millimeter-by-Millimeter in 8033 Consecutive Eyes. *Archives of Ophthalmology,* 127**,** 989-998.

SHURIN, M. R., MA, Y., KESKINOV, A. A., ZHAO, R., LOKSHIN, A., AGASSANDIAN, M. & SHURIN, G. V. 2016. BAFF and APRIL from Activin A–Treated Dendritic Cells Upregulate the Antitumor Efficacy of Dendritic Cells <em>In Vivo</em&gt. *Cancer Research,* 76**,** 4959.

SHYAMALA, K., GIRISH, H. C. & MURGOD, S. 2014. Risk of tumor cell seeding through biopsy and aspiration cytology. *Journal of International Society of Preventive & Community Dentistry,* 4**,** 5-11.

SMULSKI, C. R. & EIBEL, H. 2018. BAFF and BAFF-Receptor in B Cell Selection and Survival. *Frontiers in Immunology,* 9**,** 2285.

STEEG, P. S. 2016. Targeting metastasis. *Nature Reviews Cancer,* 16**,** 201.

SUESSKIND, D., SCHATZ, A., SCHNICHELS, S., COUPLAND, S. E., LAKE, S. L., WISSINGER, B., BARTZ-SCHMIDT, K. U. & HENKE-FAHLE, S. 2012. GDF-15: a novel serum marker for metastases in uveal melanoma patients. *Graefes Arch Clin Exp Ophthalmol,* 250**,** 887-95.

TRIOZZI, P. L., SCHOENFIELD, L., PLESEC, T., SAUNTHARARAJAH, Y., TUBBS, R. R. & SINGH, A. D. 2019. Molecular profiling of primary uveal melanomas with tumor-infiltrating lymphocytes. *OncoImmunology,* 8**,** e947169.

TRIOZZI, P. L. & SINGH, A. D. 2012. Blood biomarkers for uveal melanoma. *Future Oncol,* 8**,** 205-15.

TSAI, V. W.-W., MACIA, L., FEINLE-BISSET, C., MANANDHAR, R., ASTRUP, A., RABEN, A., LORENZEN, J. K., SCHMIDT, P. T., WIKLUND, F., PEDERSEN, N. L., CAMPBELL, L., KRIKETOS, A., XU, A., PENGCHENG, Z., JIA, W., CURMI, P. M. G., ANGSTMANN, C. N., LEE-NG, K. K. M., ZHANG, H. P., MARQUIS, C. P., HUSAINI, Y., BEGLINGER, C., LIN, S., HERZOG, H., BROWN, D. A., SAINSBURY, A. & BREIT, S. N. 2015. Serum Levels of Human MIC-1/GDF15 Vary in a Diurnal Pattern, Do Not Display a Profile Suggestive of a Satiety Factor and Are Related to BMI. *PLOS ONE,* 10**,** e0133362.

VORDERMARK, D., SAID, H. M., KATZER, A., KUHNT, T., HÄNSGEN, G., DUNST, J., FLENTJE, M. & BACHE, M. 2006. Plasma osteopontin levels in patients with head and neck cancer and cervix cancer are critically dependent on the choice of ELISA system. *BMC Cancer,* 6**,** 207.

WALLIN, U., GLIMELIUS, B., JIRSTRÖM, K., DARMANIS, S., NONG, R. Y., PONTÉN, F., JOHANSSON, C., PÅHLMAN, L. & BIRGISSON, H. 2011. Growth differentiation factor 15: a prognostic marker for recurrence in colorectal cancer. *British Journal of Cancer,* 104**,** 1619-1627.

WANG, W., YANG, X., DAI, J., LU, Y., ZHANG, J. & KELLER, E. T. 2019. Prostate cancer promotes a vicious cycle of bone metastasis progression through inducing osteocytes to secrete GDF15 that stimulates prostate cancer growth and invasion. *Oncogene,* 38**,** 4540-4559.

WANG, X., CHEN, L.-L. & ZHANG, Q. 2016a. Increased Serum Level of Growth Differentiation Factor 15 (GDF-15) is Associated with Coronary Artery Disease. *Cardiovascular Therapeutics,* 34**,** 138-143.

WANG, X., CHEN, L. L. & ZHANG, Q. 2016b. Increased Serum Level of Growth Differentiation Factor 15 (GDF-15) is Associated with Coronary Artery Disease. *Cardiovasc Ther,* 34**,** 138-43.

WEIDE, B., SCHÄFER, T., MARTENS, A., KUZKINA, A., UDER, L., NOOR, S., GARBE, C., HARTER, P. N., MITTELBRONN, M. & WISCHHUSEN, J. 2016. High GDF-15 Serum Levels Independently Correlate with Poorer Overall Survival of Patients with Tumor-Free Stage III and Unresectable Stage IV Melanoma. *J Invest Dermatol,* 136**,** 2444-2452.

WINDRICHOVA, J., FUCHSOVA, R., KUCERA, R., TOPOLCAN, O., FIALA, O., FINEK, J. & SLIPKOVA, D. 2017. MIC1/GDF15 as a Bone Metastatic Disease Biomarker. *Anticancer Research,* 37**,** 1501-1505.

WONG, Y. F., CHEUNG, T. H., LO, K. W. K., YIM, S. F. & CHUNG, T. K. H. 2006. Measurement of plasma osteopontin for detection of recurrent cervical cancer. *Cancer Research,* 66**,** 1058.

YOUDEN, W. J. 1950. Index for rating diagnostic tests. *Cancer,* 3**,** 32-35.

YU, X., ZHENG, Y., ZHU, X., GAO, X., WANG, C., SHENG, Y., CHENG, W., QIN, L., REN, N., JIA, H. & DONG, Q. 2018. Osteopontin promotes hepatocellular carcinoma progression via the PI3K/AKT/Twist signaling pathway. *Oncol Lett,* 16**,** 5299-5308.

ZHAO, D., WANG, X. & ZHANG, W. 2018a. GDF15 predict platinum response during first-line chemotherapy and can act as a complementary diagnostic serum biomarker with CA125 in epithelial ovarian cancer. *BMC Cancer,* 18**,** 328.

ZHAO, H., CHEN, Q., ALAM, A., CUI, J., SUEN, K. C., SOO, A. P., EGUCHI, S., GU, J. & MA, D. 2018b. The role of osteopontin in the progression of solid organ tumour. *Cell Death & Disease,* 9**,** 356.

ZHAO, J., LI, M., CHEN, Y., ZHANG, S., YING, H., SONG, Z., LU, Y., LI, X., XIONG, X. & JIANG, J. Elevated Serum Growth Differentiation Factor 15 Levels in Hyperthyroid Patients.

ZHAO, J., LI, M., CHEN, Y., ZHANG, S., YING, H., SONG, Z., LU, Y., LI, X., XIONG, X. & JIANG, J. 2019. Elevated Serum Growth Differentiation Factor 15 Levels in Hyperthyroid Patients. *Frontiers in Endocrinology,* 9**,** 793.